Physical Characterization of Interstellar Shocks

Bachelorarbeit aus der Physik

Vorgelegt von

Konstantin Haubner

11.10.2019

Dr. Karl Remeis-Sternwarte
Friedrich-Alexander-Universität Erlangen-Nürnberg

Betreuerin: Prof. Dr. Manami Sasaki

Abstract

Shock waves are an important phenomenon in astrophysics, since they arise in the interstellar medium (ISM) in many different context. Building on a discussion of supernova remnants (SNRs), the remains of supernova (SN) explosions, which provide one example for shocks in the ISM, a theoretical discussion of shock waves is performed in this thesis. Shock solutions are derived via a detailed analysis of neutral fluid hydrodynamics. A microscopic consideration of the behaviour of fluid particles leads to macroscopic conservation laws for mass, momentum and energy, from which sound wave solutions and then shock waves can be derived. These shocks are uniquely defined for neutral fluids, though not for collisionless plasmas, which are the usual case in astrophysical contexts. For plasmas, explicit solutions are only derived for the special case of a Maxwellian distributed electron-proton plasma in this thesis.
Shock waves, especially in SNRs, are capable of accelerating particles to relativistic energies. This makes them an ideal candidate for the explanation of the origin of cosmic rays (CR) (Helder et al., 2012). For further analyzing the acceleration of particles in SNRs, the *unicorn* code by S. Richter and F. Spanier has been used. This code performs numerical simulations of particle acceleration in shock waves inside the jets of active galactic nuclei (AGNs) (Richter and Spanier, 2016). The physical parameters of this code were adapted for describing SNRs instead of the more extreme situation inside AGN jets. Unfortunately, this approach did not yield useful results so far, and thus it is not discussed in this thesis. Still, the numerical simulation of particle acceleration in SNR shocks is an intriguing goal and will be pursued further, possibly in a following study.

Table of Contents

List of Figures

1 Introduction

Shock waves are a common feature of the interstellar medium (ISM) and arise in different contexts, e.g. supernova (SN) explosions, expanding HII regions, stellar winds or merging galaxies. A shock front is an abrupt transition between subsonic and supersonic flow of a fluid and thus leads to a discontinuous change of the fluids physical properties. Probably, the most popular example of a shock wave is the Mach cone created by an airplane (or any other object) flying with supersonic speed through the air: The plane perturbs the air as it moves through it. Since these perturbations propagate with the speed of sound, they are slower than the plane itself and the region ahead of it has no information about the incoming obstacle. This results in a rapid change of state in the gas, and thus in a shock wave.
A very important example of shocks in astrophysics are supernova remnants (SNRs). These bubble-like structures are the remains of the SNe that end the lives of stars, and consist of the fast propagating ejecta of their progenitor star. These stellar ejecta cause shock waves in the ambient ISM and heat it up. They are of special importance for astronomy, since they distribute heavy elements bred in their progenitor in the ISM and since their shock waves are capable of accelerating particles to energies of up to 100 TeV (Koyama et al., 1995). For this reason, SNRs are a main candidate for explaining the origin of the galactic share of cosmic rays (CR), high energetic charged particles that bombard the atmosphere of earth (Helder et al., 2012).

In the framework of hydrodynamics, the theoretical study of fluids, one can find shock solutions which satisfy the governing conservation laws, e.g. for mass, momentum and energy. These shocks can be considered to be large-scale sound waves, since they arise due to non-linearities in the wave equation. The non-linearities can be neglected for small-scale perturbations. For physical shocks, the second important condition for the creation of shocks are dissipative processes, which limit the steepening of the large scale waves due to non-linearities.
Based on these analyses, so-called jump conditions can be derived which describe the discontinuous change of state at the shock front for several physical quantities, e.g. density, pressure and temperature or the magnetic field strength for shocks in plasmas.

2 Motivation: Supernova Remnants

One important example for shock waves in the ISM, which will be discussed in more detail in this thesis, are the remnants of supernova explosions, abbreviated SNRs: The material which is radially ejected during a SN shocks the ambient gas and thus compresses and heats it. This results in an expanding bubble-like structure that sweeps up the surrounding ISM. An X-ray image of the Tycho remnant, which resulted from an SN observed in 1572 by Tycho Brahe, can be seen in figure 2.1.
SNRs emit photons in a variety of wavebands, most importantly radio, optical and X-ray.

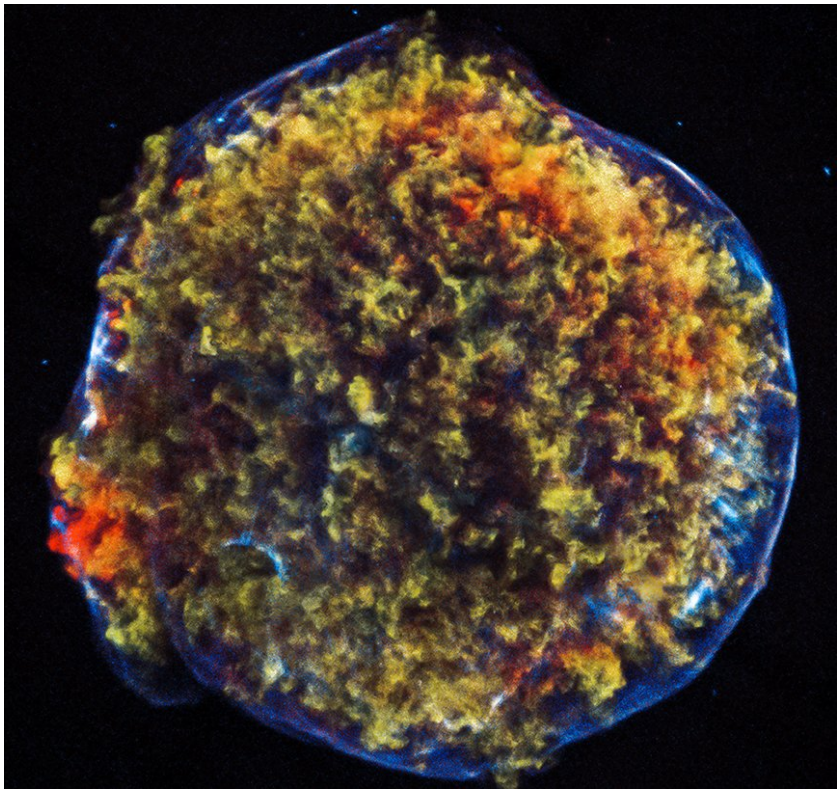

Figure 2.1: Chandra X-ray image of the Tycho supernova remnant. The forward shock in the ISM can be seen in blue, the ejected stellar material in green and red. The remnant is transitioning from free expansion to Sedov phase. Image credit: NASA/CXC/SAO

Since an SNR shock contains material of a former star, where heavier elements were bred, they are of special importance for the enrichment of the ISM with metal. Thus they influence the formation of new star and planetary systems, e.g. the solar system.

Furthermore, they are also supposed to be an important source for the acceleration of cosmic ray particles. CRs are high energetic charged particles with energies up to 10^{20} eV. They originate from the sun, galactic and even extra-galactic sources, but because of the turbulence of the galactic magnetic field, which influences their trajectories, they cannot be correlated with specific extra-solar sources. Shock acceleration in SNRs could provide an efficient mechanism for creating a large amount of the CRs from our galaxy (Helder et al., 2012).

2.1 Supernova Explosions

Supernovae are massive explosions that occur at the end of a star's lifetime. These events are the most energetic stellar processes known, with released energies in the order of magnitude of 10^{51} erg (Seward and Charles (2012), p. 98). If they happen in close proximity to earth, they can be observed with the naked eye and appear as a new star in the sky. These events build up in a relatively short time and take months or even years to fade away.
SNe are classified using their spectra and the element lines that are contained within them, i.e. Type I without hydrogen lines and type II with hydrogen lines. These types themselves have several sub-types, but in principle SNe can be distinguished via the two possible processes through which they occur:

> *Thermonuclear supernovae* are identical with type Ia. Their progenitors are binary systems of a compact white dwarf (WD) and another star of any type (even another WD). WDs are the compact remnants of stellar cores which remain after the death of a star with $M < 10M_{\odot}$. They consist of electron-degenerate matter and are stabilized against gravitational collapse through the degenerate electron pressure inside them. In a binary system, a WD will accrete mass from its companion star and so become more massive itself. Once its mass is higher than $\approx 1.44M_{\odot}$, the so-called Chandrasekhar limit, the degenerate pressure can no longer stabilize it against gravitation. The WD collapses and the resulting extreme pressure and temperature inside it cause a thermonuclear explosion which gives rise to a type Ia supernova.
>
> *Core-collapse supernovae* are the end-point of the lives of stars with $M \gtrsim 10M_{\odot}$. They do not need a companion for a SN explosion. As time goes, the star consumes the hydrogen in its core and burns it to helium. Once the hydrogen in its core is depleted, it starts burning helium, then carbon and oxygen, and so on. In the end, the star has an onion like structure with layers of different elements that get heavier towards the core. The core stops nuclear burning once it consists of iron, the most stable element. This iron core grows through the remaining fusion in the adjacent layer, until it reaches the Chandrasekhar limit and collapses into a neutron star. The gravitational energy set freely by the infalling matter causes a shock wave that ejects the surrounding layers of the star and thus gives rise to a supernova. SNe of Type II, as well as Type Ib and Ic are core-collapse SNe.

For a core-collapse supernova, the beginning of the actual SNR is marked by the shock breakout: Once the core collapses, the resulting shock inside it propagates outward from the neutron star and then accelerates the surrounding material to velocities in the order of magnitude of $10^7\,\mathrm{m\,s^{-1}}$, which causes a high Mach number shock in the ISM (Soderberg et al. (2008), Helder et al. (2012)).

2.2 Evolution of Supernova Remnants

As a simple approximation, we can assume SNe to eject stellar material radially and isotropically into all directions. These ejecta propagate through the ambient ISM and sweep up the surrounding gas, thus slowing down over time. Ahead of the ejecta, a *forward shock* is created.
The evolution of an SNR can be separated into three distinct phases: In the *free expansion phase*, the ejecta travel with a uniform velocity, until the mass of the swept up material equals the mass of the ejected material. This condition marks the beginning of the *Sedov phase* or *blast wave phase*, in which most kinetic energy has been transferred to the shock-heated shell. In this phase, the SNR expands adiabatically, as radiative processes are negligible. As the material behind the shock wave cools down, radiative processes become more and more important until the SNR enters the *radiative phase*, where radiative cooling dominates its expansion.
A schematic of the different evolutionary stages of an SNR can be seen in figure 2.2.

2.2.1 Phase I: Free Expansion Phase

Through a supernova explosion, stellar material is ejected into the ISM with energies in the range of $E_{SN} = 10^{51}\,\mathrm{erg}$. The ambient gas is swepted up by the rapidly expanding forward shock wave, which is formed ahead of the ejecta. This leaves behind a low density region in the interior of the SNR. As it grows in size, the material density inside its shell decreases until it is optically thin (Seward and Charles (2012), p. 107).
As long as the mass of the swept up material is negligible in comparison to the ejected mass M_{ej}, the velocity of the shock front V_S can be assumed to stay constant at its initial value V_0. For this reason, this phase is called the free expansion phase. The initial forward shock velocity is identical to the initial velocity of the ejected material and can be calculated via the kinetic energy E_{SN}. For an ejected mass of $M_{ej} = M_\odot$, this yields

$$V_0 = \sqrt{\frac{2E_{SN}}{M_{ej}}} = 10^9\,\mathrm{cm\,s^{-1}}. \tag{2.2.1.1}$$

This equals approximately 3% of the speed of light. For a sound speed $c_s = 10^6\,\mathrm{cm\,s^{-1}}$, this corresponds to a Mach number of $M \coloneqq V_0/c_s = 1000$.
The free expansion phase's end is defined as the point when the swept up ambient mass equals the ejected mass M_{ej}.

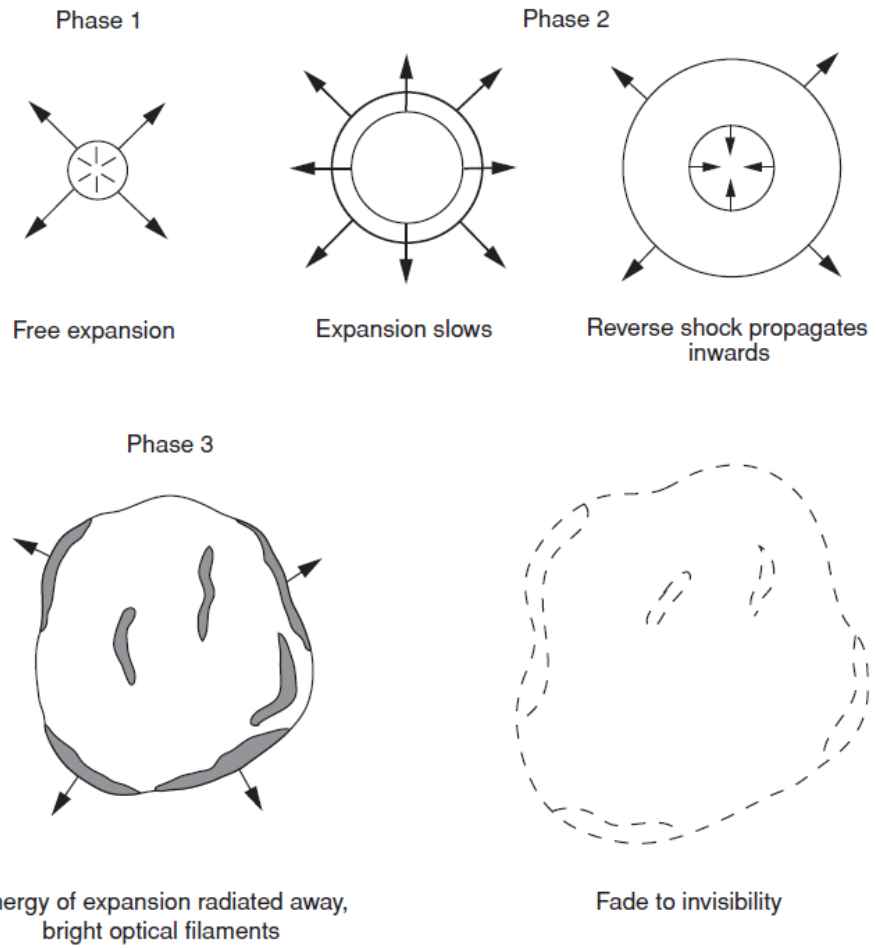

Figure 2.2: Evolution of an SNR: First it expands freely into the surrounding space. As it grows in mass, it is considerably slowed down and cools, until radiative cooling becomes efficient and further accelerates its fading away into the ISM (Seward and Charles (2012), Fig. 8.11).

2.2.2 Phase II: Sedov Phase

In the Sedov phase, enough material has been swept up in order to considerably slow down the ejected material. Since the radiation emitted by the shocked ejecta is still small compared to their internal energy, radiative processes can be neglected and the SNR can be assumed to expand adiabatically. Thus, its behaviour is only determined by its initial conditions E_{SN} and M_{ej} and the density of the ISM n. For this, we have a typical value of $n = 1\,\mathrm{cm}^{-3}$ (Helder et al., 2012).
The condition for the beginning of the Sedov phase is $M_{ej} = 4\pi R_S^3 \rho_0$, where R_S is the radius of the SNRs forward shock and ρ_0 is the mass density of the ISM: $\rho_0 \approx m_p n$, with

the proton (hydrogen) mass m_p. Thus, the remnant's radius at the beginning of the Sedov phase, R_{Sedov}, is

$$R_{Sedov} = \left(\frac{3M_{ej}}{4\pi\rho_0}\right)^{\frac{1}{3}} = 2.1\,\mathrm{pc}. \tag{2.2.2.1}$$

This corresponds to an age of the SNR of

$$t_{Sedov} = \frac{R_{Sedov}}{V_0} = 210\,\mathrm{yr}. \tag{2.2.2.2}$$

From this point on, assuming that the total explosion energy is conserved, the propagation of the forward shock in the ISM is governed by the equation

$$R_S(t) = R_{Sedov}\left(\frac{t}{t_{Sedov}}\right)^{\frac{2}{5}}. \tag{2.2.2.3}$$

Its velocity V_S is

$$V_S(t) = \frac{\mathrm{d}R_S}{\mathrm{d}t}(t) = \frac{2R_{Sedov}}{5t_{Sedov}}\left(\frac{t}{t_{Sedov}}\right)^{-\frac{3}{5}}. \tag{2.2.2.4}$$

Reverse Shock

During the Sedov phase, the velocity of the ejected material decreases faster than the velocity of the forward shock, which propagates in the ISM. Thus, the forward shock separates from the ejecta. In figure 2.1 one can see the forward shock in blue, and in contrast the ejecta in green and red. The boundary between ejected mass and the ambient gas is called the *contact discontinuity*. Additionally, the resistance of the swept up material causes another shock wave to arise in the ejecta. It is called the *reverse shock*, since it propagates from the contact discontinuity through the ejected material towards the center of the SNR. This shock's speed increases over time in the rest frame of the contact discontinuity, as the mass of the swept up material increases.
The material is only heated between the forward and the reverse shock. The material ahead of the contact discontinuity is heated and compressed by the ejecta, while the ejecta themselves are slowed down and compressed by the pressure of the interstellar gas.

Rayleigh-Taylor Instabilities

During our considerations of the evolution of SNRs we have assumed the ambient medium to be homogeneous. In nature, the ISM contains irregularities which will influence the expansion of a remnant: fluctuations of density, dense molecular clouds, the stellar winds of the progenitor star and other obstacles. This structure of the surrounding material is reflected by the appearance of SNRs, since the intensity of thermic X-ray emission is proportional to the square of the density.

Even if the initial SN explosion is completely spherical, the ejected material will fragment into so-called Rayleigh-Taylor (RT) instabilities. These instabilities occur when a heavy fluid pushes into a lighter one, e.g. a large amount of water falling through air and breaking into droplets. For an SNR, this means that at the contact discontinuity the ejected material will push into the shocked ISM ahead of it and create filamentary structures. These structures themselves are unstable and subdued to turbulences and will mix up with the ISM gas.
For an adiabatic shock, the RT instabilities are expected to extend halfway towards the forward shock front. They can even extend up to and beyond the forward shock, if energy is removed from the region behind the shock via particle acceleration. This is clearly visible for Tychos SNR in figure 2.1 (Seward and Charles (2012), p. 110).

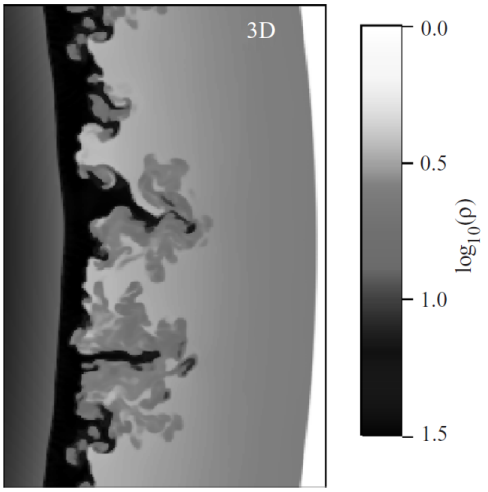

Figure 2.3: Planar slice through a 3D simulation of an SNRs shock structure. The remnant expands from left to right, density increases from white to black. The grey-white boundary to the right is the forward shock front, the grey-black boundary to the left is the reverse shock front. The ejecta are in black. One can clearly see the RT instabilities formed by them (Seward and Charles (2012), Fig. 8.14).

2.2.3 Phase III: Radiative Phase

Once the remnant has swept up enough material it will have cooled down enough for radiative processes to dominate the further evolution. This somewhat surprising result stems from the fact that after the temperature drops below approximately 2×10^5 K, enough electrons can recombine with carbon and oxygen ions for rendering UV line emission efficient. This marks the beginning of the radiative phase, which occurs at an SNR age in the order of magnitude of 10^4 years (Helder et al., 2012).
The radiative phase lasts approximately for 10^5 years. During this time, radiative cooling will give rise to bright optical filaments and reduce the internal energy of the SNR. Because

of this, it becomes fainter overall, until it becomes indistinguishable from the ambient ISM. This final process, which marks the end of an SNR, is sometimes called the *merging phase*.

2.3 Observational Signatures of Supernova Remnants

Today, we know more than 290 SNRs in the Milky-way and more than 50 in the Magellanic Clouds, and more are being discovered, even in nearby galaxies (Dubner and Giacani (2015), Seward and Charles (2012), p. 121). Each of them has a unique structure that reflects the individual initial conditions of the progenitor star and the ambient medium. Most of the galactic remnants have been discovered during radio surveys, where they could be seen as extended sources. They are distinguishable from HII regions due to their relatively flat radio spectra, which stem from a non-thermal emission process. Usually, SNRs are round in shape and appear as ring-like structures due to limb brightening, since emission mainly comes from the shock shell.
SNRs can emit photons over the entire electromagnetic spectrum, but they shine especially bright in radio and X-ray. Bright optical filaments can mainly be seen during the radiative phase, which is caused by cooling through optical and UV line emission. If there is interstellar dust near the SNR, it can be heated by the shock which can cause additional radiation in the infra-red band.

2.3.1 Radio Observations

A great majority of SNRs are radio sources. Their spectra do not stem from a thermal emission process, but are of non-thermal nature. More specifically, the radio emission from SNRs is synchrotron emission. A radio image of the Cassiopeia A remnant can be seen in figure 2.4.
An electron moving perpendicularly to a magnetic field B emits synchrotron continuum radiation. The intensity has its maximum for the critical frequency ν_c (Dubner and Giacani, 2015):

$$\nu_c = \frac{3e}{4\pi m c_0} B \left(\frac{E}{m c_0^2} \right)^2 , \tag{2.3.1.1}$$

where m is the mass and E the energy of the electron. We assume an observed critical frequency of $\nu_c = 1.5\,\mathrm{GHz}$, which lies in the radio band, and a magnetic field $B = 10\,\mu\mathrm{G}$ - typical values for B in an SNR reach from the order of magnitude of 10 to 100 μG (Reynolds et al., 2011). Radiation with such a frequency is produced by an electron with $E = 3\,\mathrm{GeV}$. This is a relativistic energy, and the question arises how electrons in an SNR acquire these energies.
To explain the radio spectra of SNR, active acceleration of electrons through the remnant is necessary (Helder et al., 2012). This happens via so-called diffusive shock acceleration, where the angular distribution of superthermal charged particles is isotropized via scattering at magnetic irregularities. Some of these particles then pass the shock front, gain

energy and their angular distribution is again isotropized, so that some of them can pass the shock again and gain even more energy. This process repeats itself until a particle has enough energy for completely leaving the SNR.

Observations of the polarization of radio photons can be used for deriving the geometry of the magnetic fields of SNRs. It is seen that young remnants have a mostly radial magnetic field structure, which can be explained via stretching of the field by the RT filaments. Older SNRs have more of a circumferential magnetic field structure, which results from compression of the ambient magnetic field by the forward shock (Helder et al., 2012).

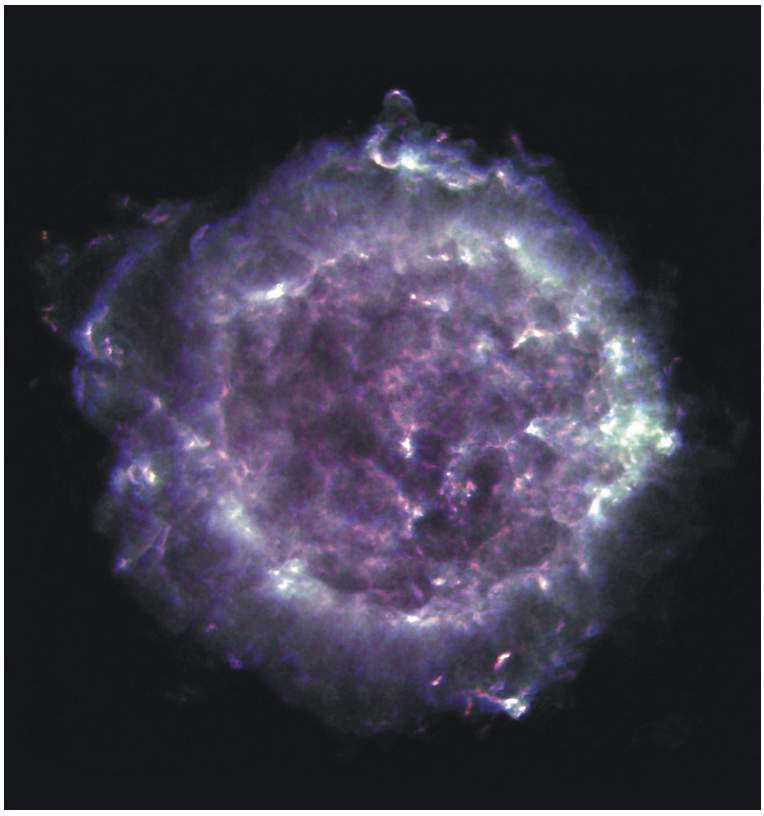

Figure 2.4: Very Large Array (VLA) radio image of the Cassiopeia A supernova remnant. Image credit: L. Rudnick, T. Delaney, J. Keohane B. Koralesky, image composite by T. Rector

2.3.2 X-ray Observations

SNRs can emit thermal X-ray photons from the shock-heated ejected material behind the forward shock. The spectra in these regions show prominent line emission and result from a plasma with temperatures of approximately 10^6 K (Seward and Charles (2012), p. 111). Remnants can also show a featureless non-thermal X-ray spectrum from the region around

the forward shock, which stems from synchrotron radiation. Synchrotron emission in the radio band corresponds to electron energies of about 1 GeV, but the presence of X-ray synchrotron radiation means that electrons are accelerated up to energies of $E = 10 - 100$ TeV. This was first observed for the remnant SN1006 by Koyama et al. (1995), and since then has also been confirmed for younger remnants like Tycho. For these younger SNRs the X-ray synchrotron emission is concentrated to narrow filaments at the forward shock front. Thermal and non-thermal spectra from the Tycho remnant can be seen in figure 2.5.

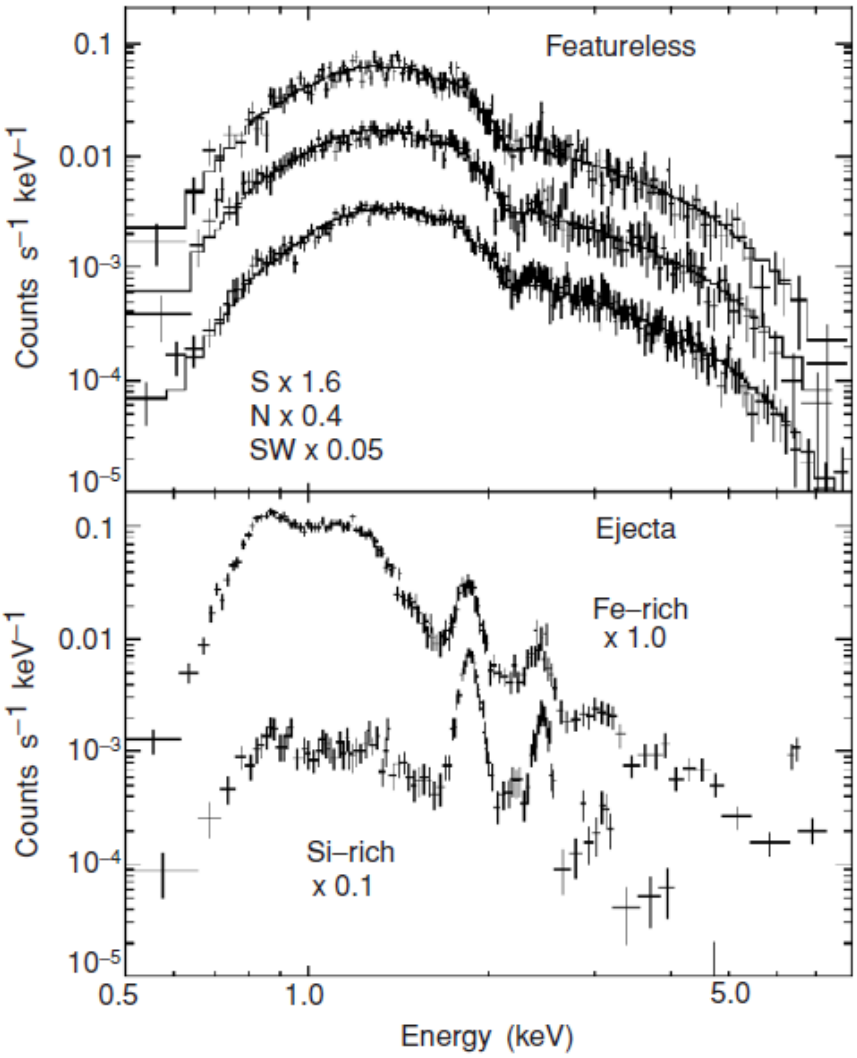

Figure 2.5: Chandra X-ray spectra from small regions of Tycho's SNR. Top: Featureless non-thermal spectra from the forward shock. Bottom: Thermal spectra from Fe-rich and Si-rich regions inside the ejecta (Seward and Charles (2012), Fig. 8.15).

3 Theoretical Discussion: Neutral Fluid Hydrodynamics

The interstellar medium (ISM) between the stars in a galaxy consists mainly of hydrogen gas and thus can be regarded as a fluid: A *fluid* is a substance that deforms continually if a shear stress is applied to it, e.g. a liquid, gas or plasma. The study of the properties and flow of fluids is the topic of *fluid hydrodynamics*, which can be used for describing shock waves in the ISM.
In this chapter, we only consider neutral fluids, i.e. fluids that consist of particles without charges. We start with the microscopic properties of fluid particles and then derive the fluid's macroscopic behaviour and finally shock solutions. In nature, astrophysical fluids are often not neutral, but plasmas, which we will analyze in chapter 4.
The discussions in this chapter are mostly based upon chapter 8, *Neutral Fluid Hydrodynamics*, of T. Padmanabhan's *Theoretical Astrophysics: Volume 1, Astrophysical Processes* (Padmanabhan, 2000).

3.1 Distribution Function and Boltzmann Equation

For describing fluids at a microscopic level, we consider the microscopic particles of which they consist, e.g. atoms or molecules. In the ISM, these are mostly hydrogen atoms, but also helium and small amounts of metals. Each particle is defined by its spatial position and momentum $(\boldsymbol{x}, \boldsymbol{p})$ inside the six-dimensional phase-space. Thus, the entire fluid can be described with the *distribution function* $f(\boldsymbol{x}, \boldsymbol{p}, t)$, which is defined via

$$\mathrm{d}N(t) = f(\boldsymbol{x}, \boldsymbol{p}, t)\mathrm{d}^3\boldsymbol{x}\mathrm{d}^3\boldsymbol{p}. \tag{3.1.0.1}$$

N is the average number of particles inside the phase-space volume element $(\mathrm{d}^3\boldsymbol{x}, \mathrm{d}^3\boldsymbol{p})$ for the time t. This means that the distribution function $f(\boldsymbol{x}, \boldsymbol{p}, t)$ gives the phase-space density of fluid particles for a certain phase-space volume element and time. Further, we demand that $f(\boldsymbol{x}, \boldsymbol{p}, t) \geq 0$, since a density cannot be negative, and $f(\boldsymbol{x}, \boldsymbol{p}, t) = 0$ for $p \longrightarrow \infty$ sufficiently rapidly for the energy of a finite number of particles to not diverge.
Macroscopic properties of the fluid can be determined from this microscopic consideration via integration of the fundamental distribution function $f(\boldsymbol{x}, \boldsymbol{p}, t)$ over the entire momentum space V_p, e.g.

the particle density $$n(\boldsymbol{x},t) = \int_{V_p} \mathrm{d}^3\boldsymbol{p} f(\boldsymbol{x},\boldsymbol{p},t), \quad (3.1.0.2)$$

the mass density $$\rho(\boldsymbol{x},t) = mn(\boldsymbol{x},t), \quad (3.1.0.3)$$

the bulk velocity $$\boldsymbol{V}(\boldsymbol{x},t) = \langle \boldsymbol{v} \rangle = n^{-1} \int_{V_p} \mathrm{d}^3\boldsymbol{p}\boldsymbol{v} f(\boldsymbol{x},\boldsymbol{p},t), \quad (3.1.0.4)$$

the average of any quantity A $$\langle A \rangle = n^{-1} \int_{V_p} \mathrm{d}^3\boldsymbol{p} A f(\boldsymbol{x},\boldsymbol{p},t), \quad (3.1.0.5)$$

where m is the mass and $\boldsymbol{v}$ is the velocity of a single particle.
The distribution function can change over time through two different physical processes: *External macroscopic force fields*, for example a gravitational field or an electromagnetic one for charged fluid particles, can cause a force $\boldsymbol{F}_{ex} = -\boldsymbol{\nabla} U_{ex}(\boldsymbol{x},t)$ on the particles, which can be derived from the external potential $U_{ex}(\boldsymbol{x},t)$.
The other process which can influence the distribution of fluid particles are *collisions* between said particles. On a fundamental level these collisions are caused by the repulsive inter-particle forces between molecules or atoms. The probability of a collision is described by the interaction cross-section $\sigma(\Omega)$, which depends on the two angular coordinates $\Omega = (\theta, \phi)$.
The evolution of $f(\boldsymbol{x},\boldsymbol{p},t)$ in time is then described via the so-called *Boltzmann equation*

$$\frac{\partial f}{\partial t} + \boldsymbol{v}\boldsymbol{\nabla} f = \boldsymbol{\nabla} U_{ex} \boldsymbol{\nabla}_{\boldsymbol{p}} f + C[f], \quad (3.1.0.6)$$

where $\boldsymbol{\nabla}_{\boldsymbol{p}} f \coloneqq \sum_i (\partial f/\partial p_i)\boldsymbol{e}_i$ and $\boldsymbol{e}_i$ the unit vector in direction i.
The two terms on the left hand side of equation (3.1.0.6) describe the change of f in time and space. The first term on the right hand side represents the influence of external force fields on f and the second term $C[f]$ is the so-called collision integral.

3.2 Collision Integral and Collisional Shocks

The collision integral in the Boltzmann equation takes the form

$$C[f_1] = \int_{V_p} \mathrm{d}^3\boldsymbol{p}_2 \int_S \mathrm{d}\Omega |\boldsymbol{v}_1 - \boldsymbol{v}_2| (f_1' f_2' - f_1 f_2)\sigma(\Omega), \quad (3.2.0.1)$$

where S is the entire solid angle of a complete sphere.
Here, $\boldsymbol{v}_1$, f_1 and f_1' denote properties of the first particle participating in the collision, and the variables with index 2 denote properties of the second particle. For collisions between identical particle types, the two types of distribution functions are identical.
The dashed f's are the distribution functions after the collision and the undashed ones the functions prior to the collision.

In general, we can distinguish two different types of fluids regarding collisions: The first one is the case of effective collisions, where the mean free path of particles $l \approx (n\sigma)^{-1}$ is very small compared to the typical size scale R of the considered system: $l \gg R$. Fluids with efficient collisions are called *collisional fluids*. The short-range interaction of particles inside them causes viscosity to arise and thus leads to dissipation. This is of special importance for the formation of physical shocks (Burgess and Scholer (2015), p. 10), as we will briefly discuss in section 3.4.4.
The second type are *collisionless fluids* with inefficient collisions. For a very large mean free path compared to the typical system scale, $l \ll R$, the collision integral in the Boltzmann equation can be neglected. Without short-range interaction between particles and without viscosity, shocks can only arise in the presence of external potentials, especially electromagnetic potentials. We will see this in our discussion of collisionless plasmas in chapter 4.

3.3 Derivation of Continuity Equations

We have defined macroscopic properties of a fluid, e.g. mass density ρ or bulk velocity $\boldsymbol{V}$, in section 3.1 via integration of the distribution function f multiplied with the corresponding microscopic quantity over the entire momentum space V_p. In this section, based on Höfner (2008), we use the same method for deriving continuity equations for macroscopic mass, momentum and energy conservation from the microscopic Boltzmann equation.

3.3.1 Moments of the Boltzmann Equation

The moments of the Boltzmann equation are formed by multiplying it with an arbitrary conserved microscopic quantity $Q(\boldsymbol{p})$ and integrating over the entire momentum space:

$$\int_{V_p} \mathrm{d}^3\boldsymbol{p} Q(\boldsymbol{p}) \left(\frac{\partial f}{\partial t} + \boldsymbol{v}\boldsymbol{\nabla} f - \boldsymbol{\nabla} U_{ex} \boldsymbol{\nabla}_{\boldsymbol{p}} f \right) = \int_{V_p} \mathrm{d}^3\boldsymbol{p} Q(\boldsymbol{p}) C[f] =: I(Q). \tag{3.3.1.1}$$

Consideration of the Collision Integral

First, we want to consider the right-hand side of this equation, the integrated collision integral $I(Q)$, and show that it equals zero. Through this we will see that the collision term vanishes for macroscopic conservation equations, regardless the efficiency of collisions. Without loss of generality, we rename the subscripts in $I(Q)$ and write

$$I(Q) \coloneqq \int_{V_p} \mathrm{d}^3\boldsymbol{p}_1 \int_{V_p} \mathrm{d}^3\boldsymbol{p}_2 \int_S \mathrm{d}\Omega Q(\boldsymbol{p}_1) |\boldsymbol{v}_1 - \boldsymbol{v}_2| (f_1' f_2' - f_1 f_2) \sigma(\Omega). \tag{3.3.1.2}$$

Switching the indices of the two particle types in the collision obviously doesn't change the value of the integral, since it's another simple renaming of variables. We get

$$I(Q) = \frac{1}{2}\int_{V_p} \mathrm{d}^3\boldsymbol{p}_1 \int_{V_p} \mathrm{d}^3\boldsymbol{p}_2 \int_S \mathrm{d}\Omega \left(Q(\boldsymbol{p}_1) + Q(\boldsymbol{p}_2)\right) |\boldsymbol{v}_1 - \boldsymbol{v}_2| (f_1' f_2' - f_1 f_2)\sigma(\Omega). \quad (3.3.1.3)$$

Due to crossing symmetry, for every collision there is an inverse collision with the same cross-section. So, we also have

$$\begin{aligned} I(Q) &= \frac{1}{2}\int_{V_p} \mathrm{d}^3\boldsymbol{p}_1' \int_{V_p} \mathrm{d}^3\boldsymbol{p}_2' \int_S \mathrm{d}\Omega' \left(Q(\boldsymbol{p}_1') + Q(\boldsymbol{p}_2')\right) |\boldsymbol{v}_1' - \boldsymbol{v}_2'| (f_1 f_2 - f_1' f_2')\sigma(\Omega') \\ &= -\frac{1}{2}\int_{V_p} \mathrm{d}^3\boldsymbol{p}_1 \int_{V_p} \mathrm{d}^3\boldsymbol{p}_2 \int_S \mathrm{d}\Omega \left(Q(\boldsymbol{p}_1') + Q(\boldsymbol{p}_2')\right) |\boldsymbol{v}_1 - \boldsymbol{v}_2| (f_1' f_2' - f_1 f_2)\sigma(\Omega), \quad (3.3.1.4) \end{aligned}$$

with $\mathrm{d}^3\boldsymbol{p}_1'\mathrm{d}^3\boldsymbol{p}_2' = \mathrm{d}^3\boldsymbol{p}_1\mathrm{d}^3\boldsymbol{p}_2$, $\mathrm{d}\Omega' = \mathrm{d}\Omega$, $\sigma(\Omega') = \sigma(\Omega)$. $|\boldsymbol{v}_1' - \boldsymbol{v}_2'| = |\boldsymbol{v}_1 - \boldsymbol{v}_2|$ follows from microscopic momentum and energy conservation.
By combining equation (3.3.1.3) and equation (3.3.1.4), we get

$$I(Q) = \frac{1}{4}\int_{V_p} \mathrm{d}^3\boldsymbol{p}_1 \int_{V_p} \mathrm{d}^3\boldsymbol{p}_2 \int_S \mathrm{d}\Omega \left(\Delta Q(\boldsymbol{p}_1) + \Delta Q(\boldsymbol{p}_2)\right) |\boldsymbol{v}_1 - \boldsymbol{v}_2| (f_1' f_2' - f_1 f_2)\sigma(\Omega), \quad (3.3.1.5)$$

with $\Delta Q(\boldsymbol{p}_1) \coloneqq Q(\boldsymbol{p}_1) - Q(\boldsymbol{p}_1')$ and $\Delta Q(\boldsymbol{p}_2)$ equivalently.
Now, if Q is a conserved quantity during the collision, i.e.

$$\Delta Q(\boldsymbol{p}_1) + \Delta Q(\boldsymbol{p}_2) = \left(Q(\boldsymbol{p}_1) + Q(\boldsymbol{p}_2)\right) - \left(Q(\boldsymbol{p}_1') + Q(\boldsymbol{p}_2')\right) = 0, \quad (3.3.1.6)$$

we get $I(Q) = 0$. This means that our further considerations regarding continuity equations are equally applicable for collisional and for collisionless fluids.

Consideration of the Moments of the Boltzmann Equation

For conserved quantities Q the moments of the Boltzmann equation now take the form

$$\int_{V_p} \mathrm{d}^3\boldsymbol{p} Q(\boldsymbol{p}) \left(\frac{\partial f}{\partial t} + \boldsymbol{v}\boldsymbol{\nabla} f - \boldsymbol{\nabla} U_{ex} \boldsymbol{\nabla}_{\boldsymbol{p}} f\right) = 0. \quad (3.3.1.7)$$

After having eliminated the collisional term, we want to further simplify the formula for the moments of the Boltzmann equation and thus make the following calculations of continuity equations easier:

Since $Q(\boldsymbol{p})$ is a conserved quantity, it is independent of t and can be pulled inside the time derivative, and since it is also independent of $\boldsymbol{x}$, it can be pulled inside the spatial divergence. Thus, we get

$$\frac{\partial}{\partial t}\left(\int_{V_p} \mathrm{d}^3\boldsymbol{p} f Q(\boldsymbol{p})\right) + \boldsymbol{\nabla}\left(\int_{V_p} \mathrm{d}^3\boldsymbol{p} f \boldsymbol{v} Q(\boldsymbol{p})\right) - \int_{V_p} \mathrm{d}^3\boldsymbol{p} Q(\boldsymbol{p}) \boldsymbol{\nabla} U_{ex} \boldsymbol{\nabla}_{\boldsymbol{p}} f = 0. \tag{3.3.1.8}$$

We notice the averages over Q and $\boldsymbol{v}Q$ according to equation (3.1.0.5) in the first two terms:

$$\frac{\partial}{\partial t}\left(n\langle Q(\boldsymbol{p})\rangle\right) + \boldsymbol{\nabla}\left(n\langle \boldsymbol{v} Q(\boldsymbol{p})\rangle\right) - \int_{V_p} \mathrm{d}^3\boldsymbol{p} Q(\boldsymbol{p}) \boldsymbol{\nabla} U_{ex} \boldsymbol{\nabla}_{\boldsymbol{p}} f = 0. \tag{3.3.1.9}$$

For simplifying the term with the external potential U_{ex}, we use partial integration:

$$-\int_{V_p} \mathrm{d}^3\boldsymbol{p} Q(\boldsymbol{p}) \boldsymbol{\nabla} U_{ex} \boldsymbol{\nabla}_{\boldsymbol{p}} f = -\left[Q(\boldsymbol{p}) \boldsymbol{\nabla} U_{ex} f\right]_{\partial V_p} + \int_{V_p} \mathrm{d}^3\boldsymbol{p} \boldsymbol{\nabla}_{\boldsymbol{p}}\left(Q(\boldsymbol{p}) \boldsymbol{\nabla} U_{ex}\right) f \tag{3.3.1.10}$$

∂V_p is the boundary of the region V_p and since f doesn't diverge, it vanishes at this boundary. So, the moments of the Boltzmann equation can be written as

$$\frac{\partial}{\partial t}\left(n\langle Q(\boldsymbol{p})\rangle\right) + \boldsymbol{\nabla}\left(n\langle \boldsymbol{v} Q(\boldsymbol{p})\rangle\right) = -n\langle \boldsymbol{\nabla}_{\boldsymbol{p}}\left(Q(\boldsymbol{p}) \boldsymbol{\nabla} U_{ex}\right)\rangle. \tag{3.3.1.11}$$

For the moment, we want to derive the continuity equations in the absence of an external potential U_{ex} interacting with the fluid. This is the case for neutral fluids without a gravitational potential. Thus, we get

$$\frac{\partial}{\partial t}\left(n\langle Q(\boldsymbol{p})\rangle\right) + \boldsymbol{\nabla}\left(n\langle \boldsymbol{v} Q(\boldsymbol{p})\rangle\right) = 0. \tag{3.3.1.12}$$

3.3.2 Mass Conservation

First, we consider the case $Q(\boldsymbol{p}) = m$, where m is the mass of a fluid particle. According to equation (3.3.1.12), we get the zeroth moment of the Boltzmann equation

$$\frac{\partial}{\partial t}\left(n\langle m\rangle\right) + \boldsymbol{\nabla}\left(n\langle m\boldsymbol{v}\rangle\right) = 0. \tag{3.3.2.1}$$

With $\langle m\rangle = m$, $\rho \coloneqq nm$ and $\boldsymbol{V} \coloneqq \langle \boldsymbol{v}\rangle$, the continuity equation for mass conservation is

$$\frac{\partial}{\partial t}\rho + \boldsymbol{\nabla}\left(\rho \boldsymbol{V}\right) = 0. \tag{3.3.2.2}$$

This equation tells us that the change in mass density ρ inside a region of the fluid over time has to equal the negative divergence of the mass flux $\boldsymbol{j} \coloneqq \rho \boldsymbol{V}$. In other words: The

mass density inside a region can only change if mass flows into or out of this region.
Since the mass of a single particle m is also conserved, this conservation law for mass density is completely equivalent to the conservation law for the particle density n:

$$\frac{\partial}{\partial t} n + \boldsymbol{\nabla} (n\boldsymbol{V}) = 0. \tag{3.3.2.3}$$

3.3.3 Momentum Conservation

For deriving a continuity equation for momentum conservation, we use $Q(\boldsymbol{p}) = m\boldsymbol{v}$ and thus the first moment of the Boltzmann equation. Notice that Q is a vector quantity this time. Because of this, we have to use the outer product $\otimes$ inside the divergence term, since $m\boldsymbol{v}$ has to be conserved for every component of $\boldsymbol{v}$ separately:

$$\frac{\partial}{\partial t} (nm\langle \boldsymbol{v} \rangle) + \boldsymbol{\nabla} (n\langle m\boldsymbol{v} \otimes \boldsymbol{v} \rangle) = 0. \tag{3.3.3.1}$$

We can separate the velocity $\boldsymbol{v} = \boldsymbol{V} + \boldsymbol{u}$ into the bulk velocity $\boldsymbol{V}$ and the random component of particle movement $\boldsymbol{u}$. By definition, we have $\langle \boldsymbol{v} \rangle = \boldsymbol{V}$ and since $\boldsymbol{u}$ describes random motion $\langle \boldsymbol{u} \rangle = \boldsymbol{0}$.
The first moment of the Boltzmann equation becomes

$$\frac{\partial}{\partial t} (\rho\boldsymbol{V}) + \boldsymbol{\nabla} (\rho(\langle \boldsymbol{V} \otimes \boldsymbol{V} \rangle + \langle \boldsymbol{u} \otimes \boldsymbol{u} \rangle + \langle \boldsymbol{V} \otimes \boldsymbol{u} \rangle + \langle \boldsymbol{u} \otimes \boldsymbol{V} \rangle)) = 0, \tag{3.3.3.2}$$

$$\frac{\partial}{\partial t} (\rho\boldsymbol{V}) + \boldsymbol{\nabla} (\rho (\boldsymbol{V} \otimes \boldsymbol{V}) + \rho\langle \boldsymbol{u} \otimes \boldsymbol{u} \rangle) = 0. \tag{3.3.3.3}$$

We define the gas pressure $P \coloneqq \frac{1}{3}\rho\langle u^2 \rangle$ and the viscous stress tensor $\overline{\overline{\pi}} \coloneqq \rho \left(\frac{1}{3}\langle u^2 \rangle \overline{\overline{I}} - \langle u \otimes u \rangle \right)$ with the unity tensor $\overline{\overline{I}}$, and thus get

$$\frac{\partial}{\partial t} (\rho\boldsymbol{V}) + \boldsymbol{\nabla} \left(\rho (\boldsymbol{V} \otimes \boldsymbol{V}) + P\overline{\overline{I}} - \overline{\overline{\pi}} \right) = 0. \tag{3.3.3.4}$$

Now, we can define the stress tensor $\overline{\overline{T}}$ as the sum behind the divergence operator: $\overline{\overline{T}} \coloneqq \rho\langle \boldsymbol{V} \otimes \boldsymbol{V} \rangle + P\overline{\overline{I}} - \overline{\overline{\pi}}$. This way, we can write the momentum conservation law as

$$\frac{\partial}{\partial t} (\rho\boldsymbol{V}) + \boldsymbol{\nabla}\overline{\overline{T}} = 0. \tag{3.3.3.5}$$

This equation describes momentum conservation, since $\rho\boldsymbol{V}$ is a momentum density and $\overline{\overline{T}}$ describes the momentum flux. For an ideal fluid without viscosity, we have $\overline{\overline{\pi}} = 0$, and thus

$$T_{ij} = \rho V_i V_j + P\delta_{ij}. \tag{3.3.3.6}$$

3.3.4 Energy Conservation

With $Q(\boldsymbol{p}) = \frac{1}{2}mv^2$, we get the second moment of the Boltzmann equation, which will lead us to energy conservation:

$$\frac{1}{2}\frac{\partial}{\partial t}\left(nm\langle v^2\rangle\right) + \frac{1}{2}\boldsymbol{\nabla}\left(nm\langle v^2\boldsymbol{v}\rangle\right) = 0 \tag{3.3.4.1}$$

Again, we separate $\boldsymbol{v}$ into the bulk velocity $\boldsymbol{V}$ and the random velocity $\boldsymbol{u}$ and get

$$\frac{1}{2}\frac{\partial}{\partial t}\left(\rho\langle V^2 + u^2 + 2\boldsymbol{V}\boldsymbol{u}\rangle\right) + \frac{1}{2}\boldsymbol{\nabla}\left(\rho\langle\left(V^2 + u^2 + 2\boldsymbol{V}\boldsymbol{u}\right)(\boldsymbol{V}+\boldsymbol{u})\rangle\right) = 0. \tag{3.3.4.2}$$

Since $\langle\boldsymbol{u}\rangle = \boldsymbol{0}$, we can drop all terms that contain this quantity only a single time. Keep in mind that again we have to use an outer product for the term that contains $\boldsymbol{u}$ two times:

$$\frac{1}{2}\frac{\partial}{\partial t}\left(\rho\langle V^2 + u^2\rangle\right) + \frac{1}{2}\boldsymbol{\nabla}\left(\rho\langle V^2\boldsymbol{V} + u^2\boldsymbol{V} + 2\boldsymbol{u}\otimes\boldsymbol{u}\boldsymbol{V} + u^2\boldsymbol{u}\rangle\right) = 0 \tag{3.3.4.3}$$

$$\frac{\partial}{\partial t}\left(\frac{1}{2}\rho\langle V^2\rangle + \frac{1}{2}\rho\langle u^2\rangle\right) + \boldsymbol{\nabla}\left(\frac{1}{2}\rho\langle V^2\boldsymbol{V}\rangle + \frac{1}{2}\rho\langle u^2\boldsymbol{V}\rangle + \rho\langle\boldsymbol{u}\otimes\boldsymbol{u}\boldsymbol{V}\rangle + \frac{1}{2}\rho\langle u^2\boldsymbol{u}\rangle\right) = 0 \tag{3.3.4.4}$$

Now, we define the internal energy per unit mass of the fluid as

$$\epsilon \coloneqq \frac{1}{2}\langle u^2\rangle = \frac{3}{2}\frac{1}{m}T \tag{3.3.4.5}$$

with the temperature T in units of energy. The kinetic energy per unit mass of the fluid is defined by combinig this internal energy with the bulk kinetic energy:

$$\bar{\epsilon} \coloneqq \frac{1}{2}m\langle V^2\rangle + m\epsilon. \tag{3.3.4.6}$$

Thus we can write

$$\frac{\partial}{\partial t}\left(n\bar{\epsilon}\right) + \boldsymbol{\nabla}\left(n\bar{\epsilon}\boldsymbol{V} + \rho\langle\boldsymbol{u}\otimes\boldsymbol{u}\rangle\boldsymbol{V} + \frac{1}{2}\rho\langle u^2\boldsymbol{u}\rangle\right) = 0, \tag{3.3.4.7}$$

where $n\bar{\epsilon}$ is the total kinetic eenrgy density of the fluid. For simplifying the divergence term, we use $\rho\langle u\otimes u\rangle = P\overline{\overline{I}} - \overline{\overline{\pi}}$ and define the conduction heat flux

$$\boldsymbol{C} \coloneqq \frac{1}{2}\rho\langle u^2\boldsymbol{u}\rangle. \tag{3.3.4.8}$$

With these considerations, the continuity equation for energy conservation is

$$\frac{\partial}{\partial t}\left(n\bar{\epsilon}\right) + \boldsymbol{\nabla}\left(n\bar{\epsilon}\boldsymbol{V} + \left(P\overline{\overline{I}} - \overline{\overline{\pi}}\right)\boldsymbol{V} + \boldsymbol{C}\right) = 0. \tag{3.3.4.9}$$

We can simplify this equation further by defining the total kinetic energy flux $\boldsymbol{q}$ as the term behind the divergence operator:

$$\frac{\partial}{\partial t}\left(n\bar{\epsilon}\right) + \boldsymbol{\nabla}\boldsymbol{q} = 0 \tag{3.3.4.10}$$

In an ideal fluid without heat conduction $\boldsymbol{C}$ or viscosity $\overline{\overline{\pi}}$, we can write the total kinetic energy flux as

$$\boldsymbol{q} = n\bar{\epsilon}\boldsymbol{V} + P\boldsymbol{V} = \left(\frac{1}{2}\langle V^2\rangle + w\right)\rho\boldsymbol{V}, \tag{3.3.4.11}$$

where w is the heat function or enthalpy per unit mass of the fluid:

$$w = \epsilon + \frac{P}{\rho} \tag{3.3.4.12}$$

3.3.5 Conservation Laws for Neutral Fluids

In total, we have derived the three continuity equations for mass, momentum and energy,

$$\frac{\partial}{\partial t}\rho + \boldsymbol{\nabla}\left(\rho\boldsymbol{V}\right) = 0, \tag{3.3.5.1}$$

$$\frac{\partial}{\partial t}\left(\rho\boldsymbol{V}\right) + \boldsymbol{\nabla}\overline{\overline{T}} = 0, \tag{3.3.5.2}$$

$$\frac{\partial}{\partial t}\left(n\bar{\epsilon}\right) + \boldsymbol{\nabla}\boldsymbol{q} = 0. \tag{3.3.5.3}$$

For an ideal fluid, one can also write the equations of mass and momentum conservation as

$$\frac{\mathrm{d}}{\mathrm{d}t}\rho + \rho\boldsymbol{\nabla}\boldsymbol{V} = 0, \tag{3.3.5.4}$$

$$\frac{\partial}{\partial t}\boldsymbol{V} + \boldsymbol{V}\boldsymbol{\nabla}\boldsymbol{V} = \frac{\mathrm{d}}{\mathrm{d}t}\boldsymbol{V} = -\frac{1}{\rho}\boldsymbol{\nabla}P. \tag{3.3.5.5}$$

For this conversion we have used the material derivative $\mathrm{d}/\mathrm{d}t \coloneqq \partial/\partial t + \boldsymbol{v}\boldsymbol{\nabla}$ and in equation (3.3.5.5) the property $\overline{\overline{\pi}} = 0$ of an ideal fluid (equation (3.3.3.6)).
For an ideal fluid, there are also no dissipative processes and fluid elements do not exchange heat during their motion. For this reason, the entropy per fluid element $s \coloneqq S/N$ is conserved:

$$\frac{\partial}{\partial t}s + \boldsymbol{V}\boldsymbol{\nabla}s = \frac{\mathrm{d}}{\mathrm{d}t}s = 0 \tag{3.3.5.6}$$

This equation is equivalent to equation (3.3.5.3).

3.4 Sound Waves and Derivation of Shock Solutions

Next, we want to study the behaviour of a *compressible fluid*, for which density variations inside it have to be considered during its flow. Such a fluid can support small-amplitude density oscillations, which are called *sound waves*. In this chapter, we want to derive a theoretical description of these waves, which will lead us to a linear solution for small-amplitude waves and a non-linear solution for large-scale waves. The non-linear wave solution will eventually give rise to shock waves.

3.4.1 Derivation of Sound Waves

For deriving a wave equation from the continuity equations for an ideal fluid, we first consider the equation of momentum conservation (3.3.5.5), which is also called *Euler's equation*. By using the identity

$$(\boldsymbol{V}\boldsymbol{\nabla})\,\boldsymbol{V} = \frac{1}{2}\boldsymbol{\nabla}V^2 - \boldsymbol{V}\times\boldsymbol{\nabla}\times\boldsymbol{V} \tag{3.4.1.1}$$

and the vorticity of the fluid $\boldsymbol{\Omega} \coloneqq \boldsymbol{\nabla}\times\boldsymbol{V}$, we can write Euler's equation as

$$\frac{\partial}{\partial t}\boldsymbol{V} - \boldsymbol{V}\times\boldsymbol{\Omega} = -\frac{1}{2}\boldsymbol{\nabla}V^2 - \frac{1}{\rho}\boldsymbol{\nabla}P. \tag{3.4.1.2}$$

We consider only irrotational flows $\boldsymbol{V} = \boldsymbol{\nabla}\psi$, so the curl of the velocity field vanishes and thus $\boldsymbol{\Omega} = \boldsymbol{0}$. Using this approach, we get

$$\frac{\partial}{\partial t}\boldsymbol{V} = -\frac{1}{2}\boldsymbol{\nabla}V^2 - \frac{1}{\rho}\boldsymbol{\nabla}P. \tag{3.4.1.3}$$

Next, we use the perturbation ansatz $P = P_0 + P'$, $\rho = \rho_0 + \rho'$ and $\boldsymbol{V} = \boldsymbol{V}'$ and linearize the Euler equation (3.4.1.3) and the equation of mass conservation (3.3.5.4). This is justified since we only consider small-amplitude disturbances of the fluid at the moment. We can drop the quadratic term inside the Euler equation - for small oscillations, the velocity will be small too, and the square term can be neglected. This gives the linearized equations

$$\frac{\partial}{\partial t}\rho' + \rho_0\boldsymbol{\nabla}\boldsymbol{V}' = 0, \qquad \frac{\partial}{\partial t}\boldsymbol{V}' + \frac{1}{\rho_0}\boldsymbol{\nabla}P' = 0. \tag{3.4.1.4}$$

Since we consider an ideal fluid, all motion inside it can be taken to be adiabatic in approximation, and thus we have $P' = (\partial P/\partial\rho)_s\rho'$, where the index s denotes a derivative at constant entropy. Using this relation, we can transform the first equation of (3.4.1.4) into

$$\frac{\partial}{\partial t}P' + \rho_0\left(\frac{\partial P}{\partial\rho}\right)_s\boldsymbol{\nabla}\boldsymbol{V}' = 0. \tag{3.4.1.5}$$

Now, we can use the irrotational ansatz $\boldsymbol{V}' = \boldsymbol{\nabla}\psi$ for the velocity field in the second equations of (3.4.1.4) and in equation (3.4.1.5) and combine these equations, which yields the wave equation

$$\frac{\partial^2}{\partial t^2}\psi - \left(\frac{\partial P}{\partial \rho}\right)_s \nabla^2\psi = 0. \tag{3.4.1.6}$$

We can further simplify this expression by defining the sound velocity c_s inside the fluid via $c_s^2 \coloneqq (\partial P/\partial\rho)_s$, which gives

$$\frac{\partial^2}{\partial t^2}\psi - c_s^2\nabla^2\psi = 0. \tag{3.4.1.7}$$

3.4.2 Physical Properties of Sound Waves

The solutions of this homogeneous partial differential equation (in one dimension) is given by the *d'Alembert solution* and yields sound waves with the shape $\psi(x,t) = f(x - c_s t) + g(x + c_s t)$, where x is the propagation direction of the waves that are moving with the velocity c_s. This solution describes a wave with two components, one propagating to the right and one propagating to the left. Since we derived this solution from the linearized wave equation, the shape of the two components of the sound wave is preserved. As we will see in chapter 3.4.4, this is not the case for the general non-linear equations, and thus the shape of large-scale oscillations changes as they propagate.
Since $\boldsymbol{V}' = \boldsymbol{\nabla}\psi$ is parallel to the x-axis, the sound waves are longitudinal with oscillations along the direction of propagation. They propagate in various physical quantities like velocity $\boldsymbol{V}$ density ρ or pressure P, though not in entropy s or vorticity $\boldsymbol{\Omega}$. These two quantities are conserved for each fluid element separately, in the case of an ideal fluid, and thus don't move relatively to the fluid.
In our consideration we assumed an ideal fluid, and because of this neglected viscosity and heat conduction. In general, these processes will have to be taken into account, which will lead to a dampening of the sound waves amplitude and dissipation of their energy as heat.

3.4.3 Supersonic Flows

In our derivation of sound waves and study of their properties we assumed that the unperturbed fluid, through which the waves are propagating, was at rest, so $\boldsymbol{V}_0 = 0$. Now we want to analyze the behaviour of sound waves in a fluid that is moving with a steady and constant velocity $\boldsymbol{V}$ from the point of view of the lab frame K. On the other hand, the frame K' with coordinates $\boldsymbol{r}'$ is co-moving with the fluid.
According to our analysis in Section 3.4.2, the oscillation of physical quantities in the co-moving frame K' will occur according to the relation $\psi \sim \exp i(\boldsymbol{k}\boldsymbol{r}' - kc_s t)$ and for $\boldsymbol{r}'$ we have $\boldsymbol{r}' = \boldsymbol{r} - \boldsymbol{V}t$. From this follows an oscillation in K according to $\psi \sim$

$\exp i(\boldsymbol{kr} - (kc_s - \boldsymbol{kV})t)$ and the group velocity of wave propagation

$$\boldsymbol{V}_g = \boldsymbol{\nabla}_{\boldsymbol{k}}\omega = \boldsymbol{V} + c_s\hat{\boldsymbol{n}}, \tag{3.4.3.1}$$

where $\hat{\boldsymbol{n}}$ is the unit vector in the direction of propagation and $\boldsymbol{\nabla}_{\boldsymbol{k}} f = \sum_i (\partial f/\partial k_i)\boldsymbol{e}_i$.
This result tells us that the net velocity of perturbation in the fluid consists of two components with respect to the lab system K: First, the sound waves are moving along with the fluid's flow with the bulk velocity $\boldsymbol{V}$, and second, the sound waves are propagating into all directions in a radial symmetry, since $\hat{\boldsymbol{n}}$ gives an arbitrary direction of propagation. Now, we want to consider a disturbance starting at point O with respect to the lab system K. After a time t_0 has passed, the disturbance will have reached every point on the edge of the circle with center at $\boldsymbol{V}t_0$ and radius $c_s t_0$. One can see a visualization of this consideration in figure 3.1.

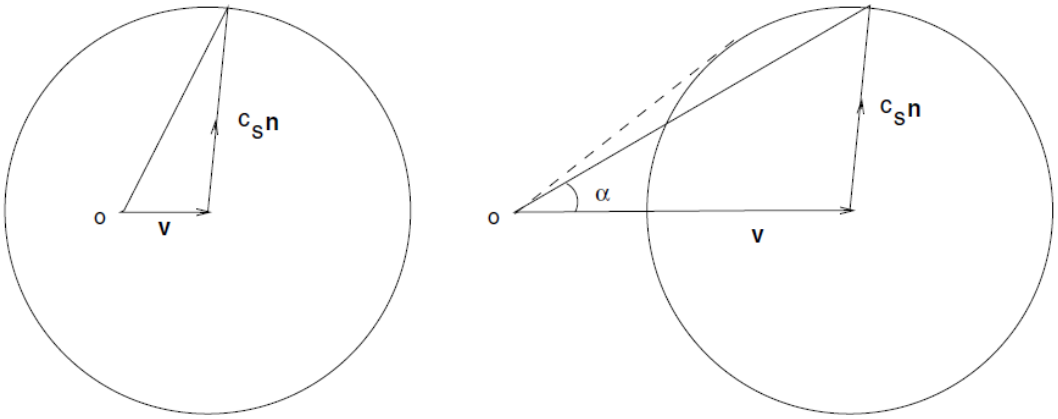

Figure 3.1: Propagation of a perturbation starting at point O in a fluid moving with velocity $\boldsymbol{V}$. After a finite time, the perturbation reaches every point on the circles' boundaries. Left: *Subsonic flow* with $v < c_s$, where the perturbation reaches every point of the fluid after some time. Right: *Supersonic flow* with $v > c_s$, where the perturbation can't reach the upstream fluid (Padmanabhan (2000), Fig. 8.1).

We have to distinguish two different results of this analysis:
The fluid is moving *subsonically* for the case $V < c_s$. This means that the vector $\hat{\boldsymbol{n}}c_s$ is longer than the vector $\boldsymbol{V}$ and the perturbation will propagate from point O into every direction and eventually reach every point of the fluid.
On the other hand, for *supersonic* fluids we have $V > c_s$ and thus a perturbation starting at point O cannot reach any other point of the fluid. The direction into which the disturbance propagates can only lie within a cone with vertex O and a semi-vertical angle of $\alpha \approx c_s/V$.
The existence of supersonic flows has important consequences for our study of fluid hydrodynamic: We consider an object inside a fluid, which rests with respect to the lab frame

while the fluid flows around it with supersonic speed. The object perturbs the fluid around itself, but the perturbations can only reach the downstream regions of the fluid. *Downstream* means in direction of the fluid flow and *upstream* the opposite direction. Thus, the fluid in the upstream region stays unperturbed and contains no information about the body, until it flows around it and gets perturbed in the downstream region.

3.4.4 Steepening of Sound Waves

In section 3.4.1 we derived a linear wave equation from the continuity equations of an ideal fluid, using the assumption of small-amplitude disturbances through the waves. The d'Alembert-solutions of this wave equation lead to $\boldsymbol{V}$, ρ and P each depending on $(x \pm c_s t)$ alone. Because of this, these three quantities could be expressed in terms of each other and the derived sound waves didn't change their shape over the course of time.
The linearization approach is no longer valid when we want to consider perturbations with large amplitudes. In particular, we have to bear in mind that the sound velocity c_s is proportional to $\rho^{1/3}$, and thus the propagation speed of the wave is higher in regions of higher density. This will lead to a distortion and steepening of the wave's shape over time, since high-density regions will overtake low-density regions. To understand this process in detail, we have to consider the non-linear mass conservation equation (3.3.5.1) and Euler equation (3.4.1.3):

$$\frac{\partial \rho}{\partial t} + \frac{\partial (\rho V)}{\partial x} = 0, \qquad \frac{\partial V}{\partial t} + \frac{V \partial V}{\partial x} + \frac{1}{\rho}\frac{\partial P}{\partial x} = 0 \tag{3.4.4.1}$$

While keeping the analysis general, we assumed a sound wave propagating along the x-axis, so we could write the velocity field as $V_x = V(x,t)$, $V_y = 0$ and $V_z = 0$ and replace the divergence operators with one-dimensional spatial derivations.
An ideal fluid's flow is adiabatic in the absence of shock waves, and if the fluid is homogeneous at some initial instance, it's flow is also isentropic. In this case, the pressure inside the fluid depends on the density alone: $P = P(\rho)$. On the other hand, we consider a flow with a velocity $V_x = V(\rho)$ that also depends only on the density. Using these assumptions, we can write the equations (3.4.4) as

$$\frac{\partial \rho}{\partial t} + \frac{\mathrm{d}(\rho V)}{\mathrm{d}\rho}\frac{\partial \rho}{\partial x} = 0, \qquad \frac{\partial V}{\partial t} + \left(V + \frac{1}{\rho}\frac{\mathrm{d}P}{\mathrm{d}V}\right)\frac{\partial V}{\partial x} = 0. \tag{3.4.4.2}$$

Now we can use implicit derivation, i.e. $(\partial x/\partial t)_\rho = -[(\partial \rho/\partial t)/(\partial \rho/\partial x)]$ and equivalently for ρ substituted with V and thus derive from these equations

$$\left(\frac{\partial x}{\partial t}\right)_\rho = \frac{\mathrm{d}(\rho V)}{\rho} = V + \rho\frac{\mathrm{d}V}{\mathrm{d}\rho}, \qquad \left(\frac{\partial x}{\partial t}\right)_V = V + \frac{1}{\rho}\frac{\mathrm{d}P}{\mathrm{d}V}. \tag{3.4.4.3}$$

Since we have $\rho = \rho(V)$, it follows that $(\partial x/\partial t)_\rho = (\partial x/\partial t)_V$ and we can equate the two

former expressions. With further simplification, we arrive at

$$V = \pm \int \mathrm{d}\rho \frac{c_s}{\rho} = \pm \int \frac{\mathrm{d}P}{\rho c_s}. \tag{3.4.4.4}$$

We can substitute the derived expression for $\mathrm{d}P$ back into the second equation of (3.4.4.3), which leads us to

$$\left(\frac{\partial x}{\partial t}\right)_V = V \pm c_s(V) \tag{3.4.4.5}$$

Via integration, we obtain the relation

$$x = t[v \pm c_s(V)] + f(V), \tag{3.4.4.6}$$

where $f(V)$ is an arbitrary function of V, that has to be determined through the initial conditions.
This equation determines the velocity V, and thus also the sound velocity c_s, as an implicit function of the spatial coordinate x and time t. This means, that the propagation speed of a disturbance in the fluid is different for different regions in the fluid.
This result for the non-linear wave equation for large-amplitude perturbations is qualitatively different from the solution for small-scale perturbations in section 3.4.1. Still, the propagation velocity of any perturbation has two components in the lab frame K: The bulk velocity V of the fluids flow and the sound velocity c_s of the perturbation in the rest frame of the co-moving fluid. In particular, the latter one, $c_s = c_s(\rho)$, depends on the density of the fluid and in general increases with density.
Hence, regions of higher density inside the fluid will slowly overtake regions of lower density with time, and thus cause a steepening of the density profile between such two regions. This change will continue and, in theory, cause the density to become a multi-valued function of the spatial coordinate after a finite duration of time.
Such a solution would be unphysical and cannot be the case in reality: Instead of actually becoming multi-valued, the density profile forms a sharp discontinuity at the transition point between the high- and low-density region. This discontinuity is called a *shock front*. A visualization of the steepening of a large-scale shock wave over time can be seen in figure 3.2.

Limiting of Steepening

In reality, one limiting factor for the steepening of waves is the viscosity of the fluid, which we neglected due to our assumption of an ideal fluid. Viscosity arises due to particle collisions and leads to dissipation. This can exemplary be seen using Burger's equation

$$\frac{\partial u}{\partial t} + u\frac{\partial u}{\partial x} = \epsilon \frac{\partial^2 u}{\partial t^2}, \tag{3.4.4.7}$$

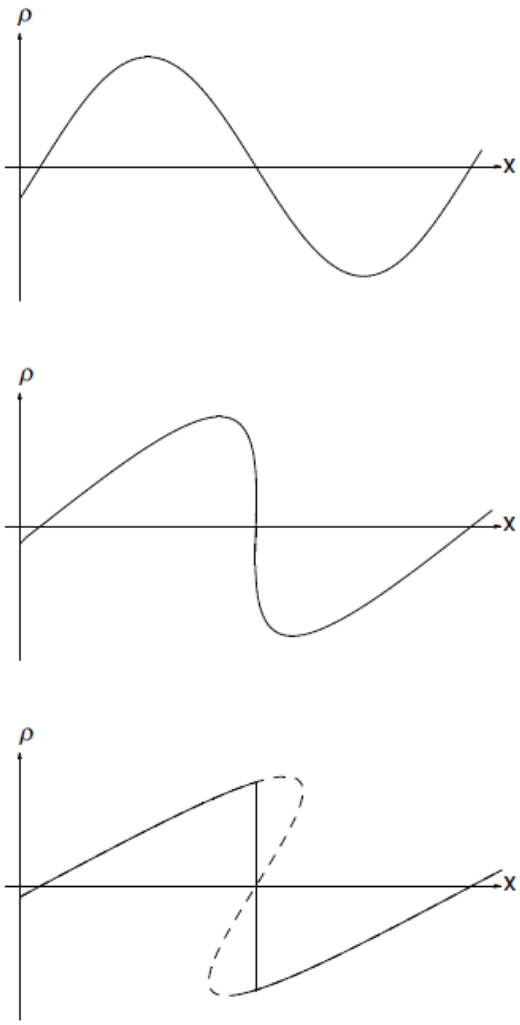

Figure 3.2: Steepening of a large-amplitude density wave. Time evolves from top to bottom. In the last graphic, one can see that $\rho(x)$ would become a multi-valued function (dashed line), if it wasn't limited to a discontinuity (Padmanabhan (2000), Fig. 8.4).

where $u = u(x,t)$ is an arbitrary quantity which experiences wave steepening due to non-linearity. On the right-hand side, we have the viscous term with parameter ϵ. For a small value of ϵ, this term will stay unimportant for small gradients of u, but become bigger for increasing gradients and eventually limit the steepening of the wave. Thus, u will not become a multi-valued function and the system remains physical. In our limit of an ideal fluid, with $\epsilon \longrightarrow 0$, the viscous term will limit the steepening to a discontinuous shock front (Burgess and Scholer (2015), pp. 5, 6).

Location of the Discontinuity

The discontinuity's location inside the fluid can be easily calculated. We label the time of the shock's formation t_0. At the time $t = t_0$, the gradient of velocity V at the location of the shock front x_0 becomes infinite, and so we have $(\partial x/\partial V)_t = 0$. On the other hand, the point x_0 is a point of inflection for the function $x(V)$. This is described by $(\partial^2 x/\partial V^2)_t = 0$, and we get the requirements that determine the location and time of formation of the discontinuity:

$$\left(\frac{\partial x}{\partial V}\right)_t = 0, \qquad \left(\frac{\partial^2 x}{\partial V^2}\right)_t = 0 \tag{3.4.4.8}$$

Together with equation (3.4.4.6) and some additional information about the considered fluid, these expressions allow the calculation of the shock's initial position.
For the special case of a discontinuity formed between moving and stationary fluid, these conditions have to be modified. Since the velocity will vanish everywhere on the stationary side, the second derivative of x need not vanish. Instead, the condition $(\partial c/\partial t)_v = 0$ has to be satisfied at the shock's surface.

3.4.5 Shock Waves

A shock is an abrupt transition between a supersonic and a subsonic flow. They arise when a solid obstacle moves with supersonic speed relative to a fluid, as discussed in section 3.4.3. In the lab frame K, this can be the case for a stationary fluid and an obstacle moving with supersonic speed, or a stationary obstacle and a supersonic flow of the fluid around it. For the obstacle to move through the fluid, the fluid ahead of it has to be diverted around it, which will cause a transition from the supersonic flow ahead of the obstacle to a subsonic flow adjacent to it. This has to be the case, since otherwise the pressure force of the obstacle, which propagates with the speed of sound, would be swept downstream and could not interact with the fluid ahead of the obstacle. Thus, the fluid's flow could not be diverted around the obstacle. This rapid transition from supersonic to subsonic flow caused by the obstacle gives rise to a shock wave. The shock wave can be regarded as a large-amplitude oscillation with a discontinuity in its density profile at the transition point, as derived in section 3.4.4.
In this section, we want to analyze the effect of a shock wave on the physical quantities density ρ, pressure P and temperature T. For doing so, we approximate the shock front as planar. In the case of SNRs, whis would be justified if a small enough region of their sphere surface is considered. We study the fluid's behaviour in the rest frame of the shock front, thus the shock front is considered to be stationary and, for an SNR, the interstellar medium surrounding it is flowing perpendicularly through the shock front. This shock geometry can also be seen in figure 3.3. We define the gas to the left of the shock front as the ISM gas, and thus as the upstream region from which gas is flowing with supersonic speed through the shock front to the right. The physical quantities on the left-hand side are denoted with an index 1: ρ_1, P_1 and T_1. The region to the right of the shock front

is the downstream region, in which the shocked gas is moving to the right with subsonic speed in the rest-frame of the shock front. The quantities in this region have the index 2: ρ_2, P_2 and T_2.

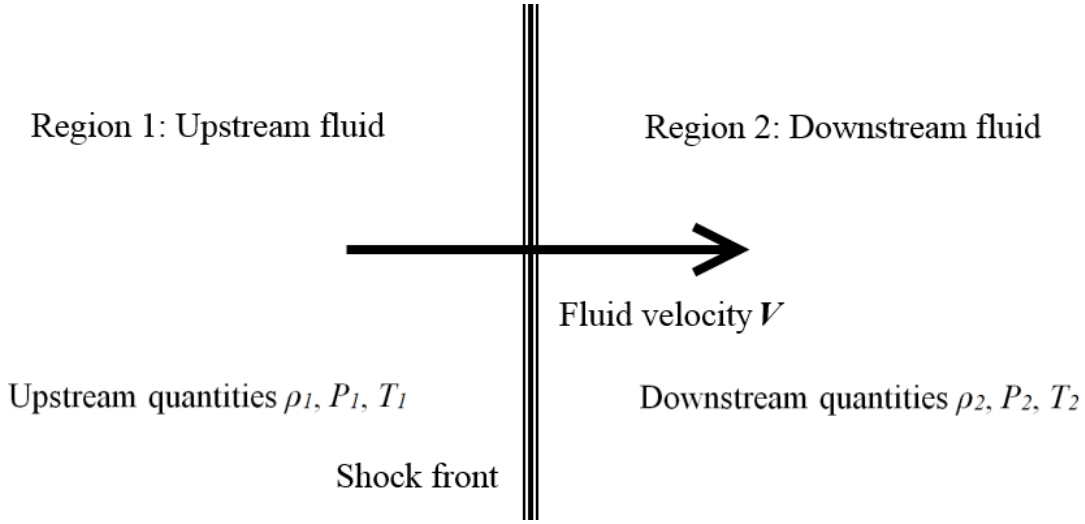

Figure 3.3: Geometry of a shock transition in a neutral fluid in the shock front's rest frame. Left: Unshocked upstream region of the fluid. Right: Shocked downstream region.

The physical quantities in the shocked and un-shocked region are related by the continuity equations for mass (3.3.5.1), momentum (3.3.5.2) and energy (3.3.5.3). We can integrate these conservation laws over a suitable volume which spans the discontinuity, and thus derive jump conditions for the shock front. Since mass, momentum and energy density don't change over time on each side of the shock, we can drop the time derivatives. Then, we get the conservation of mass as

$$\rho_1 V_1 = \rho_2 V_2 = j, \tag{3.4.5.1}$$

with the mass flux j as the mass passing through a unit surface per unit of time. The conservation of momentum flux can be written as

$$P_1 + \rho_1 V_1^2 = P_2 + \rho_2 V_2^2. \tag{3.4.5.2}$$

Since we consider an ideal fluid, we can drop the heat conduction flux and viscosity in the equation of energy conservation and use equation (3.3.4.11), which expresses the kinetic energy flux through the enthalpy w. This way, the conservation of energy at the shock front becomes

$$w_1 + \frac{1}{2}V_1^2 = w_2 + \frac{1}{2}V_2^2. \tag{3.4.5.3}$$

This set of jump conditions is called the *Rankine-Hugoniot relations*.

We consider a poltropic fluid, i.e. a fluid where the relation $PV_S^\gamma = \text{const.}$ holds. Here, V_S is the volume of the gas and γ is called the polytropic index. Then we can express the enthalpy w via the formula

$$w = \frac{\gamma}{\gamma - 1}\frac{P}{\rho} = \frac{\gamma}{\gamma - 1}k_B T, \tag{3.4.5.4}$$

and thus relate our conservation laws to the temperature T of the gas.

We solve this system of equations via straightforward algebraic manipulation and express the solutions in terms of the upstream Mach number $M_1 \coloneqq V_1/c_s$. What we get are formulas for the relations between the value of a physical quantity in the shocked and in the unshocked region, e.g. $\rho_2/\rho_1 =: r$, V_2/V_1 etc., where r is called the *shock compression ratio*. We find that

$$r \coloneqq \frac{\rho_2}{\rho_1} = \frac{V_1}{V_2} = \frac{(\gamma+1)M_1^2}{(\gamma+1)+(\gamma-1)(M_1^2-1)}, \tag{3.4.5.5}$$

$$\frac{P_2}{P_1} = \frac{(\gamma+1)+2\gamma(M_1^2-1)}{(\gamma+1)}, \tag{3.4.5.6}$$

$$\frac{T_2}{T_1} = \frac{[(\gamma+1)+2\gamma(M_1^2-1)][(\gamma+1)+(\gamma-1)(M_1^2-1)]}{(\gamma+1)^2 M_1^2}. \tag{3.4.5.7}$$

Since the gas on the left-hand side of the shock front, which is denoted with index 1, is unshocked and flows with supersonic speed to the right, its Mach number is bigger than 1: $M_1 > 1$. Hence the mass density, pressure and temperature of the shocked gas is larger than that of the unshocked gas. One can see the plotted results in figure 3.4 and figure 3.5. On the other hand, the velocity of the unshocked gas is higher than that of the shocked: $\rho_2 > \rho_1$, $P_2 > P_1$, $T_2 > T_1$, but $V_2 < V_1$. Thus, the shock wave compresses and heats up the ISM as it sweeps it up, and slows it down in respect to the rest-frame of the shock front - in the rest-frame of the ISM, this corresponds to the shock wave entraining the ambient gas.
Now we want to analyze the derived ratios quantitatively for the limit of the strongest shock $M_1 \longrightarrow \infty$. The compression ratio becomes $r = \rho_2/\rho_1 = (\gamma+1)/(\gamma-1)$. For a mono-atomic gas, the polytropic index is $\gamma = 5/3$, and thus the maximum possible compression ratio is $r = 4$. In the same limit, we don't get a finite value for the ratios of pressure and temperature: P_2/P_1 and T_2/T_1 diverge in the limit of the strongest shock.

Our derivation of the jump conditions relies on conservation of mass, momentum and energy being applicable at the shock front. Though this condition is usually satisfied for the first two of these quantities, there are several processes which can change the total energy at the shock front, especially in the case of an SNR. First, chemical or nuclear reactions can occur around the shock front and thus energy can be added to the flow of the fluid. Second, once the shock wave has cooled down enough and entered the radiative

phase, as described in section 2.2.3, radiative cooling will start to become efficient and the shock front will loose energy through radiation. Third, particles can be accelerated to superthermal speeds at the shock front and diffuse ahead of it. Then they will preheat the incoming upstream gas and thus remove energy from the shock itself. This will lead to a thickening of the shock front and it can no longer be approximated as a discontinuity. As we have seen, this process happens in SNRs, too, due to their ability to accelerate particles to high energies.
When the conservation of mass, momentum and energy each hold and none of these effects are relevant, the shock is called adiabatic. For SNRs, the phase of adiabatic expansion is the Sedov phase, as described in section 2.2.2.

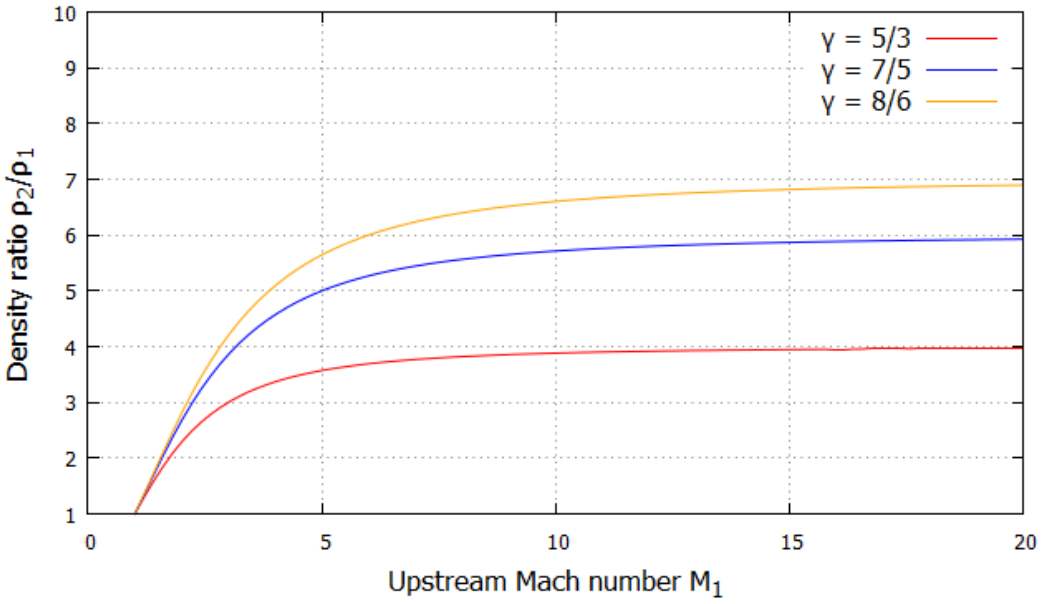

Figure 3.4: Shock compression ratio $r = \rho_2/\rho_1$ in dependence of the upstream Mach number M_1 for different polytropic indices γ. For the limit of very high Mach numbers, the compression ratio approaches a finite value. This value itself approaches 1 for higher polytropic indices.

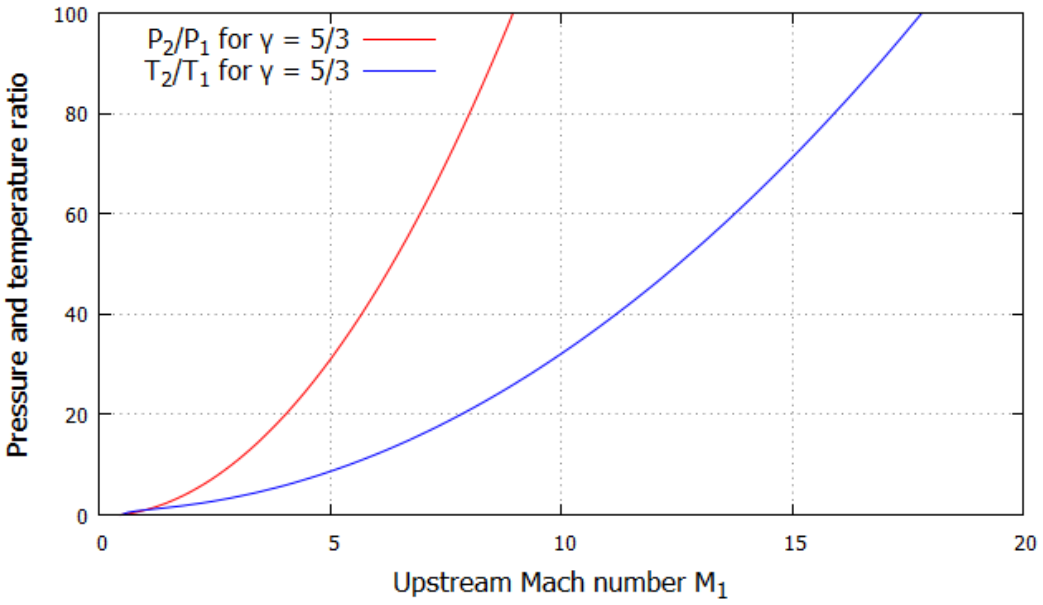

Figure 3.5: Ratio between the upstream and downstream values for pressure, P_2/P_1, and temperature, T_2/T_1, in dependance of the upstream Mach number M_1. These ratios diverge for higher Mach numbers.

4 Theoretical Discussion: Collisionless Plasmas

In our analysis in chapter 3 we only considered neutral fluids and thus neglected the influence of electric and magnetic fields. For these types of fluid, small-scale dissipative processes are necessary to limit the steepening of sound-waves and thus allowing physical shocks to form. These dissipative processes arise due to particle collisions inside the fluid. Now, we consider an interstellar hydrogen gas with a typical density $n \approx 1\,\mathrm{cm}^3$ and a shock wave propagating through it with velocity $V \approx 1000\,\mathrm{km\,s}^{-1}$. This yields a mean free path for particles $l \approx 1 \times 10^{15}\,\mathrm{m}$ (Sasaki, 2019). Such a large mean free path renders collisions utterly inefficient, and hence dissipative processes via viscosity too.
The fluids of interstellar shock-waves are in general *collisionless plasmas*, and thus the participating particles are charged and the collective motion of the plasma results in electric and magnetic fields. The interaction of the fluid's particles with these electromagnetic potentials provides the short-range coupling necessary for shock-waves with dissipative features (Burgess and Scholer (2015), p. 11).
The main source for our analysis of shocks in collisionless plasmas in this chapter is *Collisionless Shocks in Space Plasmas* by Burgess and Scholer, especially chapter 2.2 *Shock conservation relations*.

4.1 Vlasov-Maxwell Equations

As for neutral fluids, the starting point for our analysis of collisionless plasmas is the microscopic Boltzmann equation

$$\frac{\partial f}{\partial t} + \boldsymbol{v}\boldsymbol{\nabla} f = \boldsymbol{\nabla} U_{ex} \boldsymbol{\nabla}_{\boldsymbol{p}} f + C[f]. \tag{4.1.0.1}$$

We drop the collision integral, since the mean free path of particles in interstellar plasmas renders collisions inefficient. On the other hand, we can no longer drop the term which describes an external potential, since we consider charged particles. Their charges q are influenced by the electric field $\boldsymbol{E}$ and the magnetic field $\boldsymbol{B}$. Then the external potential U_{ex} is the electromagnetic potential, which leads to the Lorentz-Coulomb force on a single particle

$$-\boldsymbol{\nabla} U_{ex} = q(\boldsymbol{E} + \boldsymbol{v} \times \boldsymbol{B}). \tag{4.1.0.2}$$

As before, $\boldsymbol{v}$ is the velocity of a fluid particle. Inserted into the Boltzmann equation, the electromagnetic potential yields the *Vlasov equation* (4.1.0.3). Combined with the four Maxwell equations, we get the *Vlasov-Maxwell system of equations*, which is sufficient for describing a collisionless plasma:

$$\frac{\partial f_j}{\partial t} + \boldsymbol{v}\boldsymbol{\nabla} f_j + q_j(\boldsymbol{E} + \boldsymbol{v} \times \boldsymbol{B})\boldsymbol{\nabla}_{\boldsymbol{p}} f_j = 0, \tag{4.1.0.3}$$

$$\boldsymbol{\nabla}\boldsymbol{E} = \frac{1}{\epsilon_0}\sum_j q_j \int_{V_p} \mathrm{d}^3\boldsymbol{p} f_j, \tag{4.1.0.4}$$

$$\boldsymbol{\nabla}\boldsymbol{B} = 0, \tag{4.1.0.5}$$

$$\boldsymbol{\nabla} \times \boldsymbol{E} = -\frac{\partial \boldsymbol{B}}{\partial t}, \tag{4.1.0.6}$$

$$\boldsymbol{\nabla} \times \boldsymbol{B} = \mu_0 \sum_j q_j \int_{V_p} \mathrm{d}^3\boldsymbol{p}\boldsymbol{v} f_j + \frac{1}{c_0^2}\frac{\partial \boldsymbol{E}}{\partial t}. \tag{4.1.0.7}$$

c_0 is the speed of light in vacuum, ϵ_0 is the vacuum permittivity and μ_0 is the vacuum permeability, with $c_0^2 = 1/(\epsilon_0\mu_0)$. The subscript j denotes the the particle species, e.g. electrons e, protons p or ions i. This becomes especially important, since these particle types can not only differ in distribution, mass and absolute charge, but also in charge sign. Further, we define the *electric charge density*

$$\rho_{em,j} \coloneqq \int_{V_p} \mathrm{d}^3\boldsymbol{p} q_j f_j, \tag{4.1.0.8}$$

and the *electric charge flux*

$$\boldsymbol{j}_{em,j} \coloneqq \int_{V_p} \mathrm{d}^3\boldsymbol{p} q_j \boldsymbol{v} f_j. \tag{4.1.0.9}$$

4.2 Derivation of Continuity Equations

As we did with the Boltzmann equation in section 3.3, we can derive macroscopic continuity equations for mass, momentum and energy by taking the moments of the Vlasov equation:

$$\frac{\partial}{\partial t}\left(n\langle Q(\boldsymbol{p})\rangle\right) + \boldsymbol{\nabla}\left(n\langle \boldsymbol{v}Q(\boldsymbol{p})\rangle\right) = -n\langle \boldsymbol{\nabla}_{\boldsymbol{p}}\left(Q(\boldsymbol{p})\boldsymbol{\nabla}U_{ex}\right)\rangle. \tag{4.2.0.1}$$

Since the external potential doesn't vanish in the case of plasmas, but is the electromagnetic potential, our new conservation laws will be modified by terms for the electromagnetic momentum density and energy density.
From our analysis in the previous chapter, we already know the left-hand terms of the

above equation for the first three moments of the Vlasov equation and can simply read them from section 3.3.5. Thus, we only have to analyze the right-hand terms here.

4.2.1 Mass Conservation

The conservation of mass for a collisionless plasma is described by the zeroth moment of the Vlasov equation,

$$\frac{\partial}{\partial t}\rho_j + \boldsymbol{\nabla}\left(\rho_j \boldsymbol{V}\right) = -n_j \langle \boldsymbol{\nabla}_{\boldsymbol{p}}\left(m_j \boldsymbol{\nabla} U_{ex}\right)\rangle. \tag{4.2.1.1}$$

We insert the electromagnetic potential on the right-hand side, which becomes

$$-n\langle \boldsymbol{\nabla}_{\boldsymbol{p}}\left(m_j \boldsymbol{\nabla} U_{ex}\right)\rangle = n_j m_j q_j \langle \boldsymbol{\nabla}_{\boldsymbol{p}}(\boldsymbol{E} + \boldsymbol{v} \times \boldsymbol{B})\rangle. \tag{4.2.1.2}$$

The electric field $\boldsymbol{E}$ doesn't depend on the momentum $\boldsymbol{p}$ and the product $\boldsymbol{v} \times \boldsymbol{B}$ is perpendicular to $\boldsymbol{p}$, since $\boldsymbol{v} \parallel \boldsymbol{p}$. Hence, equation (4.2.1.2) equals zero and the mass continuity equation is

$$\frac{\partial}{\partial t}\rho_j + \boldsymbol{\nabla}\left(\rho_j \boldsymbol{V}\right) = 0. \tag{4.2.1.3}$$

As one can see, the conservation law for mass in a collisionless plasma is identical to the one in a neutral fluid. The only difference is the consideration of different particles species in this case, but since mass is conserved for each particle type separately, it is easily shown through summing up over j that the total fluid mass also is conserved:

$$\frac{\partial}{\partial t}\rho + \boldsymbol{\nabla}\left(\rho \boldsymbol{V}\right) = 0. \tag{4.2.1.4}$$

4.2.2 Momentum Conservation

Our starting point for deriving the momentum conservation law is the first moment of the Vlasov equation,

$$\frac{\partial}{\partial t}\left(\rho_j \boldsymbol{V}\right) + \boldsymbol{\nabla}\left(\overline{\overline{T}}_j\right) = -n_j \langle \boldsymbol{\nabla}_{\boldsymbol{p}}\left(m_j \boldsymbol{v} \boldsymbol{\nabla} U_{ex}\right)\rangle. \tag{4.2.2.1}$$

We use the product rule on the right-hand side, and since $\boldsymbol{\nabla}_{\boldsymbol{p}}(m_j \boldsymbol{v}) = 1$, we have

$$\begin{aligned} n_j \langle \boldsymbol{\nabla}_{\boldsymbol{p}}\left(m_j \boldsymbol{v} \boldsymbol{\nabla} U_{ex}\right)\rangle &= n_j q_j \langle \boldsymbol{E} + \boldsymbol{v} \times \boldsymbol{B}\rangle \\ &= \langle \rho_{em,j} \boldsymbol{E} + \boldsymbol{j}_{em,j} \times \boldsymbol{B}\rangle. \end{aligned} \tag{4.2.2.2}$$

Again, we can sum up over all particle species and the momentum conservation law for a collisionless plasma becomes

$$\frac{\partial}{\partial t}\left(\sum_j \rho_j \boldsymbol{V}\right) + \boldsymbol{\nabla}\left(\sum_j \overline{\overline{T}}_j\right) = \langle \rho_{em}\boldsymbol{E} + \boldsymbol{j}_{em} \times \boldsymbol{B}\rangle. \tag{4.2.2.3}$$

Next, we want to express the right-hand side of this equation purely in terms of divergences and time derivatives of $\boldsymbol{E}$ and $\boldsymbol{B}$ and thus combine it with the left-hand side. First, we use the Ampère-Maxwell law (4.1.0.7) for substituting the electric charge flux $\boldsymbol{j}_{em}$ and further include a vanishing term for symmetry reasons via Kelvin's law (4.1.0.5):

$$\boldsymbol{j}_{em} \times \boldsymbol{B} = \left(\frac{1}{\mu_0}\boldsymbol{\nabla} \times \boldsymbol{B} - \epsilon_0 \frac{\partial \boldsymbol{E}}{\partial t}\right) \times \boldsymbol{B} + \frac{1}{\mu_0}\left(\boldsymbol{\nabla}\boldsymbol{B}\right)\boldsymbol{B}. \tag{4.2.2.4}$$

Similarly, we use Gauss's law (4.1.0.4) for expressing the charge density ρ_{em} via the electric field and add a vanishing term with Faraday's law (4.1.0.6). We get

$$\rho_{em}\boldsymbol{E} = \epsilon_0 \left(\boldsymbol{\nabla}\boldsymbol{E}\right)\boldsymbol{E} + \epsilon_0 \left(\boldsymbol{\nabla} \times \boldsymbol{E} + \frac{\partial \boldsymbol{B}}{\partial t}\right) \times \boldsymbol{E}. \tag{4.2.2.5}$$

Now, we combine the two above equations. Using the relation $\partial/\partial t(\boldsymbol{E} \times \boldsymbol{B}) = \boldsymbol{E} \times \partial\boldsymbol{B}/\partial t + \partial\boldsymbol{E}/\partial t \times \boldsymbol{B}$ and taking into account the vector product's anti-symmetry during our transformations, we have

$$\begin{aligned}\rho_{em}\boldsymbol{E} + \boldsymbol{j}_{em} \times \boldsymbol{B} = &- \frac{\partial}{\partial t}\left[\epsilon_0 \boldsymbol{E} \times \boldsymbol{B}\right] - \epsilon_0\left[\boldsymbol{E} \times (\boldsymbol{\nabla} \times \boldsymbol{E}) - (\boldsymbol{\nabla}\boldsymbol{E})\boldsymbol{E}\right] \\ &- \frac{1}{\mu_0}\left[\boldsymbol{B} \times (\boldsymbol{\nabla} \times \boldsymbol{B}) - (\boldsymbol{\nabla}\boldsymbol{B})\boldsymbol{B}\right].\end{aligned} \tag{4.2.2.6}$$

The terms to the right of the time derivative can be written as the divergence of the so-called electromagnetic stress tensor:

$$\epsilon_0\left[\boldsymbol{E} \times (\boldsymbol{\nabla} \times \boldsymbol{E}) - (\boldsymbol{\nabla}\boldsymbol{E})\boldsymbol{E}\right] + \frac{1}{\mu_0}\left[\boldsymbol{B} \times (\boldsymbol{\nabla} \times \boldsymbol{B}) - (\boldsymbol{\nabla}\boldsymbol{B})\boldsymbol{B}\right] = \boldsymbol{\nabla}\overline{\overline{T}}_{em}. \tag{4.2.2.7}$$

The tensor $\overline{\overline{T}}_{em}$ is defined as

$$\overline{\overline{T}}_{em} \coloneqq \frac{1}{2}\overline{\overline{I}}\left(\epsilon_0 \boldsymbol{E}^2 + \frac{1}{\mu_0}\boldsymbol{B}^2\right) - \epsilon_0 \boldsymbol{E} \otimes \boldsymbol{E} - \frac{1}{\mu_0}\boldsymbol{B} \otimes \boldsymbol{B}. \tag{4.2.2.8}$$

These transformations allow us to write the momentum continuity equation for a collisionless plasma as

$$\begin{aligned}&\frac{\partial}{\partial t}\left(\sum_j \rho_j \boldsymbol{V} + \langle \epsilon_0 \boldsymbol{E} \times \boldsymbol{B} \rangle\right) \\ &\quad + \boldsymbol{\nabla}\left(\sum_j \overline{\overline{T}}_j + \left\langle \overline{\overline{I}} \frac{\epsilon_0 \left(\boldsymbol{E}^2 + c_0^2 \boldsymbol{B}^2\right)}{2} - \epsilon_0 \boldsymbol{E} \otimes \boldsymbol{E} - \frac{1}{\mu_0} \boldsymbol{B} \otimes \boldsymbol{B} \right\rangle\right) = 0.\end{aligned} \tag{4.2.2.9}$$

As we can see now, the term $\epsilon_0 \boldsymbol{E} \times \boldsymbol{B}$ describes the electromagnetic momentum density, while the stress tensor $\overline{\overline{T}}_{em}$ describes the electromagnetic momentum flux. The mechanic momentum density is no longer a conserved quantity - instead, the total momentum density is conserved.

4.2.3 Energy Conservation

We take the second moment of the Vlasov equation for deriving the energy conservation law for collisionless plasmas:

$$\frac{\partial}{\partial t}\left(n_j \overline{\epsilon}_j\right) + \boldsymbol{\nabla} \boldsymbol{q}_j = -n_j \left\langle \boldsymbol{\nabla}_{\boldsymbol{p}} \left(\frac{1}{2} m_j v^2 \boldsymbol{\nabla} U_{ex}\right)\right\rangle. \tag{4.2.3.1}$$

Again, we use the product rule for derivations on the right-hand term, which yields

$$\begin{aligned}-n_j \left\langle \boldsymbol{\nabla}_{\boldsymbol{p}} \left(\frac{1}{2} m_j v^2 \boldsymbol{\nabla} U_{ex}\right)\right\rangle &= n_j q_j \left\langle \boldsymbol{v} \left(\boldsymbol{E} + \boldsymbol{v} \times \boldsymbol{B}\right)\right\rangle \\ &= \left\langle \boldsymbol{j}_{em,j} \boldsymbol{E} \right\rangle.\end{aligned} \tag{4.2.3.2}$$

Thus, energy conservation in a collisionless plasma is described by the equation

$$\frac{\partial}{\partial t}\left(\sum_j n_j \overline{\epsilon}_j\right) + \boldsymbol{\nabla}\left(\sum_j \boldsymbol{q}_j\right) = \left\langle \boldsymbol{j}_{em} \boldsymbol{E} \right\rangle. \tag{4.2.3.3}$$

As in the case of momentum conservation, we want to eliminate the electric current $\boldsymbol{j}_{em}$ and express the electromagnetic term solely through $\boldsymbol{E}$ and $\boldsymbol{B}$. First, we use the Ampère-Maxwell law (4.1.0.7):

$$\begin{aligned}\boldsymbol{j}_{em} \boldsymbol{E} &= \left(\frac{1}{\mu_0} \boldsymbol{\nabla} \times \boldsymbol{B} - \epsilon_0 \frac{\partial}{\partial t} \boldsymbol{E}\right) \boldsymbol{E} \\ &= \frac{1}{\mu_0} \left(\boldsymbol{\nabla} \times \boldsymbol{B}\right) \boldsymbol{E} - \frac{\epsilon_0}{2} \frac{\partial}{\partial t} \boldsymbol{E}^2,\end{aligned} \tag{4.2.3.4}$$

where we used the chain rule for the electric term in the second transformation. Next, we use the identity $\boldsymbol{\nabla}(\boldsymbol{E}\times\boldsymbol{B}) = \boldsymbol{B}(\boldsymbol{\nabla}\times\boldsymbol{E}) - \boldsymbol{E}(\boldsymbol{\nabla}\times\boldsymbol{B})$ and Faraday's law (4.1.0.6), and thus get

$$\begin{aligned}\boldsymbol{j}_{em}\boldsymbol{E} &= \frac{1}{\mu_0}\left[\boldsymbol{B}(\boldsymbol{\nabla}\times\boldsymbol{E}) - \boldsymbol{\nabla}(\boldsymbol{E}\times\boldsymbol{B})\right] - \frac{\epsilon_0}{2}\frac{\partial}{\partial t}\boldsymbol{E}^2 \\ &= \frac{1}{\mu_0}\left(-\boldsymbol{B}\frac{\partial}{\partial t}\boldsymbol{B}\right) - \frac{1}{\mu_0}\boldsymbol{\nabla}(\boldsymbol{E}\times\boldsymbol{B}) - \frac{\epsilon_0}{2}\frac{\partial}{\partial t}\boldsymbol{E}^2 \\ &= -\frac{1}{\mu_0}\boldsymbol{\nabla}(\boldsymbol{E}\times\boldsymbol{B}) - \frac{\epsilon_0}{2}\frac{\partial}{\partial t}\boldsymbol{E}^2 - \frac{1}{2\mu_0}\frac{\partial}{\partial t}\boldsymbol{B}^2.\end{aligned} \tag{4.2.3.5}$$

Plugged into equation (4.2.3.6), the conservation law for energy in a collisionless plasma becomes

$$\frac{\partial}{\partial t}\left(\sum_j n_j\bar{\epsilon}_j + \left\langle\frac{\epsilon_0\left(\boldsymbol{E}^2 + c_0^2\boldsymbol{B}^2\right)}{2}\right\rangle\right) + \boldsymbol{\nabla}\left(\sum_j \boldsymbol{q}_j + \left\langle\frac{1}{\mu_0}\boldsymbol{E}\times\boldsymbol{B}\right\rangle\right) = 0. \tag{4.2.3.6}$$

The electric energy density is described by the term $(\epsilon_0/2)\boldsymbol{E}^2$ and the magnetic energy equivalently by $(1/(2\mu_0))\boldsymbol{B}^2$. The electromagnetic energy flux is described by the so-called Poynting vector $\boldsymbol{S} \coloneqq (1/\mu_0)\boldsymbol{E}\times\boldsymbol{B}$.

4.2.4 Continuity Equations for Collisionless Plasmas

In total, we have the three continuity equations for mass, momentum and energy in a collisionless plasma:

$$\frac{\partial}{\partial t}\rho_j + \boldsymbol{\nabla}\left(\rho_j\boldsymbol{V}\right) = 0, \tag{4.2.4.1}$$

$$\begin{aligned}&\frac{\partial}{\partial t}\left(\sum_j \rho_j\boldsymbol{V} + \langle\epsilon_0\boldsymbol{E}\times\boldsymbol{B}\rangle\right) \\ &\quad + \boldsymbol{\nabla}\left(\sum_j \overline{\overline{T}}_j + \left\langle\overline{\overline{I}}\frac{\epsilon_0\left(\boldsymbol{E}^2 + c_0^2\boldsymbol{B}^2\right)}{2} - \epsilon_0\boldsymbol{E}\otimes\boldsymbol{E} - \frac{1}{\mu_0}\boldsymbol{B}\otimes\boldsymbol{B}\right\rangle\right) = 0,\end{aligned} \tag{4.2.4.2}$$

$$\frac{\partial}{\partial t}\left(\sum_j n_j\bar{\epsilon}_j + \left\langle\frac{\epsilon_0\left(\boldsymbol{E}^2 + c_0^2\boldsymbol{B}^2\right)}{2}\right\rangle\right) + \boldsymbol{\nabla}\left(\sum_j \boldsymbol{q}_j + \left\langle\frac{1}{\mu_0}\boldsymbol{E}\times\boldsymbol{B}\right\rangle\right) = 0. \tag{4.2.4.3}$$

Additionaly, the Vlasov equation fulfills the relation

$$\frac{\partial}{\partial t}\int_{V_p} \mathrm{d}^3\boldsymbol{p}\phi(f) + \boldsymbol{\nabla}\int_{V_p} \mathrm{d}^3\boldsymbol{p}\boldsymbol{v}\phi(f) = 0, \tag{4.2.4.4}$$

where $\phi(f)$ is an arbitrary function that satisfies $\boldsymbol{v}\phi(f) \longrightarrow 0$ for $v \longrightarrow \pm\infty$. One can derive this relation by multiplying the Vlasov equation with $\partial\phi/\partial f$ and integrating over the entire momentum space.

4.3 Shock Conservation Relations

Now we want to analyze the behaviour of these conservation laws at a shock and thus relate the values of different physical quantities on both sides of the shock front, as we did in section 3.4.5 for neutral fluids. Again, we choose the rest frame of the shock front. We define the x-axis as perpendicular to the shock surface and consider a planar shock, where all quantities only depend on x.
As we did for the velocity $\boldsymbol{v}$, we separate the electric and magnetic field into an averaged macroscopic part and a fluctuating microscopic part: $\boldsymbol{E} = \langle\boldsymbol{E}\rangle + \delta\boldsymbol{E}$ and $\boldsymbol{B} = \langle\boldsymbol{B}\rangle + \delta\boldsymbol{B}$. The averages of the fluctuating fields equal zero. We write the shock conservation relations in integral form, to keep the consideration general at the moment. Dropping the time derivatives in our continuity equations, since macroscopic quantities are time-stationary on both sides of the shock front, we have

$$\int_{V_p} \mathrm{d}^3\boldsymbol{p}v_x f_j = const., \tag{4.3.0.1}$$

$$\sum_j \int_{V_p} \mathrm{d}^3\boldsymbol{p}m_j\boldsymbol{v}v_x f_j + \frac{\epsilon_0}{2}(\langle\boldsymbol{E}\rangle^2 + c_0^2\langle\boldsymbol{B}\rangle^2 + \langle\delta\boldsymbol{E}\rangle^2 + c_0^2\langle\delta\boldsymbol{B}\rangle^2)\boldsymbol{e}_x$$
$$- \epsilon_0(\langle\boldsymbol{E}\rangle\langle E_x\rangle + c_0^2\langle\boldsymbol{B}\rangle\langle B_x\rangle + \langle\boldsymbol{E}\delta E_x\rangle + c_0^2\langle\boldsymbol{B}\delta B_x\rangle) = const., \tag{4.3.0.2}$$

$$\sum_j \int_{V_p} \mathrm{d}^3\boldsymbol{p}\frac{1}{2}m_j v^2 v_x f_j + \frac{1}{\mu_0}(\langle\boldsymbol{E}\rangle \times \langle\boldsymbol{B}\rangle + \langle\boldsymbol{\delta E} \times \boldsymbol{\delta B}\rangle)\boldsymbol{e}_x = const., \tag{4.3.0.3}$$

where $\boldsymbol{e}_x$ is the unit vector parallel to the x-axis. From equation (4.2.4.4), we get

$$\sum_j \int_{V_p} \mathrm{d}^3\boldsymbol{p}v_x\langle\phi(f)\rangle = const. \tag{4.3.0.4}$$

Additionally, we can use the Maxwell equations for deriving further constrains on the E and B field's behaviour at the shock. From Faraday's law (4.1.0.6) we learn that the electric fields tangential component (relative to the shock) is conserved, and from Kelvin's law (4.1.0.5) that the magnetic field's normal component is conserved:

$$\langle E_t \rangle = const. \tag{4.3.0.5}$$

$$\langle B_x \rangle = const. \tag{4.3.0.6}$$

If there are no gradients or turbulances far from the shock, we can further assume the Coulomb-Lorentz force vanishes at this boundary:

$$\langle \boldsymbol{E} \rangle + \boldsymbol{V} \times \langle \boldsymbol{B} \rangle = 0, \qquad x \longrightarrow \pm\infty. \tag{4.3.0.7}$$

Combined with equation (4.3.0.5), this yields

$$[\boldsymbol{V} \times \boldsymbol{B}]_t = const. \tag{4.3.0.8}$$

The system of equations from equation (4.3.0.1) to equation (4.3.0.8) are the conservation relations for a shock front in a collisionless plasma. Other than the Rankine-Hugoniot relations in the case of a neutral fluid, this set of equations does not have a unique solution for the relations between upstream and downstream quantities. This is due to the quantity $\phi(f)$ in equation (4.3.0.4) being arbitrary, which basically allows an infinite number of solutions for this problem.
Thus, we need further assumptions about the nature of the considered fluid and the shock wave, if we want to derive actual jump conditions. One should bear in mind that these assumptions are obviously not fulfilled for every shock in a collisionless plasma, especially not in every real astrophysical context.
First, we assume an electron-proton plasma, which has a drifting Maxwellian distribution. Electrons and ions move with a common bulk velocity V, but the electron temperature T_e and the ion temperature T_i are distinct. The ion distribution function is

$$f_i = \frac{n_i}{(2\pi v_i^2)^{3/2}} \exp\left(-\frac{(\boldsymbol{v} - \boldsymbol{V})^2}{2v_i^2}\right), \tag{4.3.0.9}$$

and the electron distribution function has a similar form. v_i is the ions' thermal velocity, which is defined via

$$v_{i,e} = \left(\frac{k_B T_{i,e}}{m_{i,e}}\right)^{1/2}. \tag{4.3.0.10}$$

From this point on, additionally to the particle species index, we use the subscripts u and d for denoting upstream and downstream quantities in the fluid. Since we have already assumed the absence of turbulences far from the shock for equation (4.3.0.7), the microscopic fluctuating fields $\langle \delta \boldsymbol{E} \rangle$ and $\langle \delta \boldsymbol{B} \rangle$ can be neglected everywhere outside the shock transition

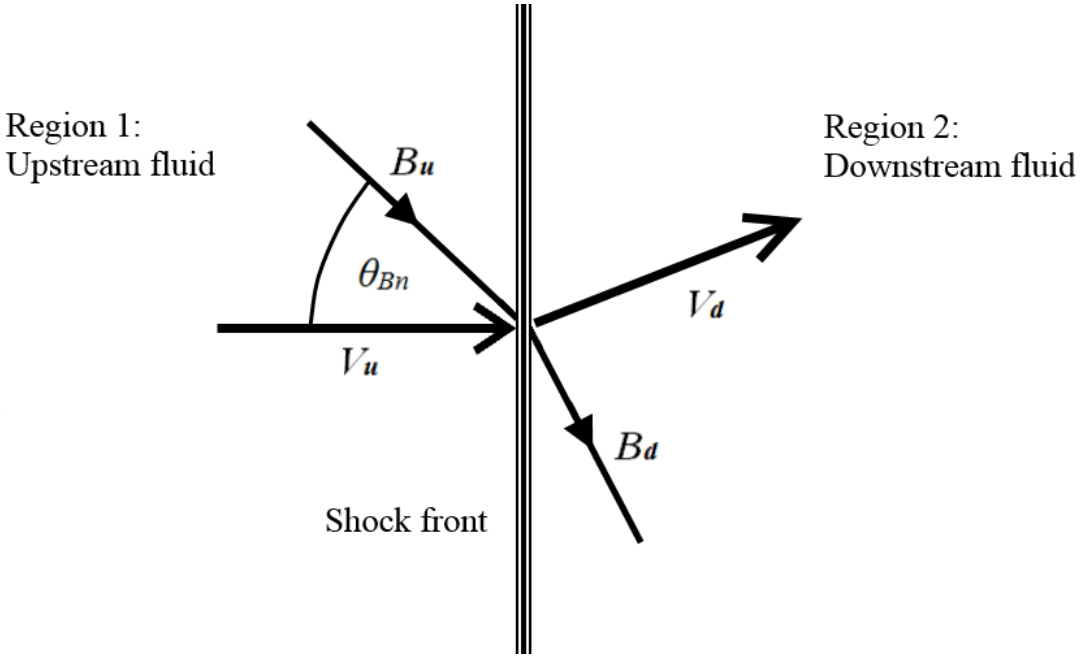

Figure 4.1: Geometry of a shock transition in a collisionless plasma in the shock front's rest frame. Left: Unshocked upstream region of the fluid. Right: Shocked downstream region. Other than in the case of neutral fluids, the flow direction of the fluid can be changed through the shock.

itself, and we drop the average notation for the electromagnetic fields $\boldsymbol{E}$ and $\boldsymbol{B}$.
Now, we choose a rest frame in which the upstream bulk velocity of the fluid is directed normal to the fluid. The coordinate system is defined so that $\boldsymbol{V}_u = V_u \boldsymbol{e}_x$ and $\boldsymbol{B}_u$ both lie in the x-z-plane. With equation (4.3.0.7) we have

$$\boldsymbol{E}_u = V_u B_{uz} \boldsymbol{e}_y \tag{4.3.0.11}$$

with $\boldsymbol{e}_y$ the unit vector parallel to the y-axis.
The angle between the upstream magnetic field and the normal vector of the shock front is called θ_{Bn}, thus $B_x = B_u \cos\theta_{Bn}$ and $B_{uz} = B_u \sin\theta_{Bn}$. Bear in mind that $B_x = B_{ux} = B_{dx}$, since the magnetic field's normal component is conserved through the shock (equation (4.3.0.6)). The geometry of the considered shock transition can be seen in figure 4.1.
We make two further assumptions: First, we assume that there are no charges or current far from the shock on both sides of the shock front, thus $n_{eu,d} = n_{iu,d} = n_{u,d}$ and $\boldsymbol{V}_{eu,d} = \boldsymbol{V}_{iu,d} = \boldsymbol{V}_{u,d}$. Second, the downstream quantities $\boldsymbol{V}_d$ and $\boldsymbol{B}_d$ are assumed to lie in the x-z plane, just like $\boldsymbol{V}_u$ and $\boldsymbol{B}_u$. This is called the coplanarity theorem.
We use equation (4.3.0.1), the x component of equation (4.3.0.2) and equation (4.3.0.3), and get

$$n_u V_u = n_d V_d, \tag{4.3.0.12}$$

$$n_u \left(\bar{v}_u^2 + V_u^2\right) + \frac{B_{uz}^2}{2\mu_0 m_i} = n_u \left(\bar{v}_d^2 + V_{dx}^2\right) + \frac{B_{dz}^2}{2\mu_0 m_i}, \tag{4.3.0.13}$$

$$n_u V_u \left(5\bar{v}_u^2 + V_u^2\right) + \frac{2V_u B_{uz}^2}{\mu_0 m_i} = n_d V_{dx} \left(5\bar{v}_d^2 + V_{dx}^2 + V_{dz}^2\right) + \frac{2V_{dx} B_{dz}^2}{\mu_0 m_i} - \frac{2V_{dz} B_x B_{dz}}{\mu_0 m_i}, \tag{4.3.0.14}$$

where we've defined

$$\bar{v}^2 = v_i^2 + \frac{m_e}{m_i} v_e^2, \tag{4.3.0.15}$$

and dropped all terms of order m_e/m_i or $V_{u,d}^2/c_0^2$, which corresponds to the assumption of a non-relativistic shock.
We can use the y component of equation (4.3.0.8) for deriving

$$V_u B_{uz} = V_{dx} B_{dz} - V_{dz} B_x \tag{4.3.0.16}$$

and the z component of equation (4.3.0.2) for deriving

$$\frac{B_{uz} B_x}{\mu_0 m_i} = \frac{B_{dz} B_x}{\mu_0 m_i} - n_d V_{dx} V_{dz}. \tag{4.3.0.17}$$

Next, we define the Alfvén Mach number M_A, which relates the bulk velocity to the propagation speed of ion oscillations, and the so-called plasma beta β, which is the ratio of thermic to magnetic pressure. We also use the shock compression ratio r, which is defined exactly as for neutral fluids:

$$r \coloneqq \frac{n_d}{n_u} = \frac{V_u}{V_{dx}}, \tag{4.3.0.18}$$

$$M_A = \frac{V_u}{B_u/\sqrt{\mu_0 n_u m_i}}, \tag{4.3.0.19}$$

$$\beta_u = \frac{n_u k_B (T_{iu} + T_{eu})}{B_u^2/(2\mu_0)}. \tag{4.3.0.20}$$

Now, we can use equation (4.3.0.12) for solving the equations (4.3.0.16) and (4.3.0.17). This yields the results

$$\frac{B_{dz}}{B_{uz}} = \frac{r(M_A^2 - \cos^2\theta_{Bn})}{M_A^2 - r\cos^2\theta_{Bn}}, \tag{4.3.0.21}$$

$$\frac{V_{dz}}{V_u} = \frac{\sin\theta_{Bn}\cos\theta_{Bn}(r-1)}{M_A^2 - r\cos^2\theta_{Bn}}. \tag{4.3.0.22}$$

The first equation relates the z components of the downstream and the upstream magnetic field. A plot for different angles θ_{Bn} can be seen in figure 4.2. Since $r > 1$, the downstream magnetic field is stronger than the upstream one: The shock compresses the magnetic field. For the limit of very high Mach numbers $M_A \longrightarrow \infty$, we have $B_{dz}/B_{uz} = r$, which equals a ratio of four to one, as we will see in the following considerations.
The second equation relates the z component of the downstream bulk velocity to the upstream bulk velocity. Its plot can be seen in figure 4.3. Since the upstream bulk velocity is parallel to the x axis, its z component equals zero and the ratio V_{dz}/V_u in principle represents the deflection of the fluid's flow at the shock surface. For very high Mach numbers, this ratio approaches zero, thus the faster the fluid's supersonic upstream flow, the less it is deflected.

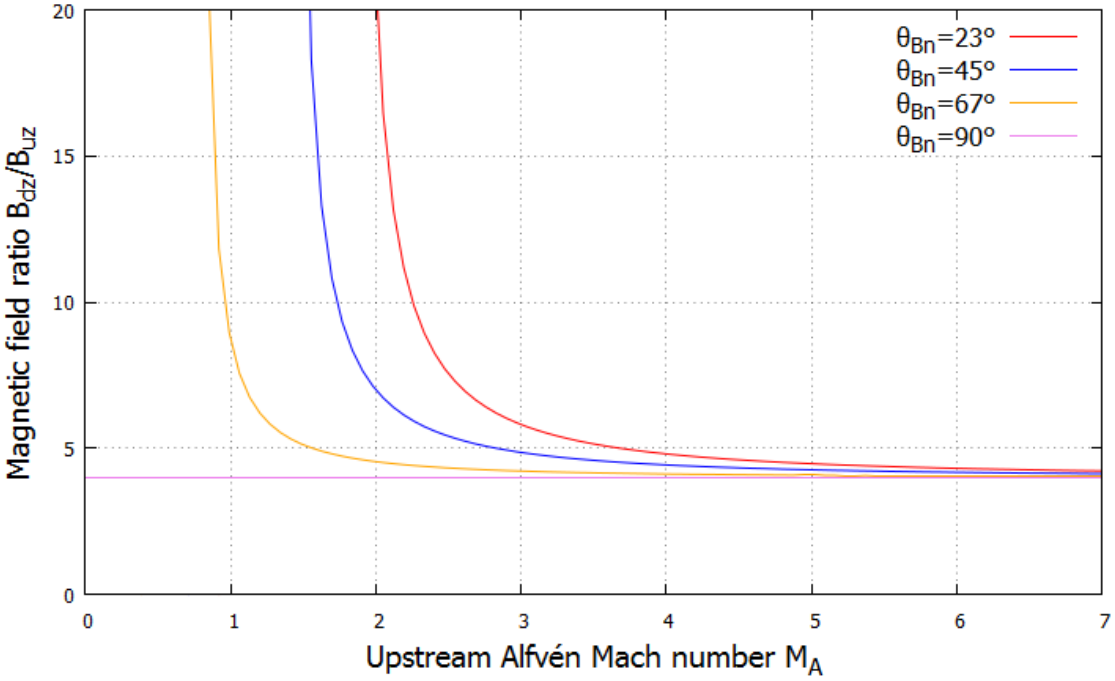

Figure 4.2: Magnetic field compression ratio B_{dz}/B_{uz} in dependance of the Alfvén Mach Number M_A for different angles θ_{Bn}. For the limit of very high Mach numbers, the ratio approaches the maximum density compression ratio $r = 4$. For $\theta_{Bn} = 0$, which corresponds to an upstream magnetic field parallel to the shock surface, the ratio is constant and independent of M_A.

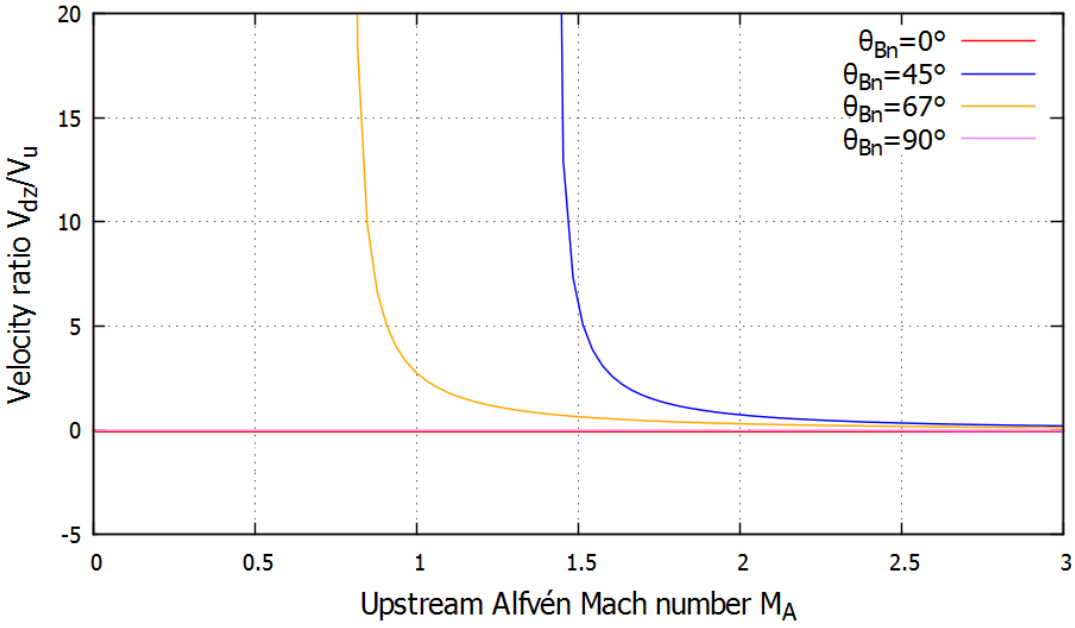

Figure 4.3: Deflection of the fluid flow V_{dz}/V_u in dependance of the Alfvén Mach Number M_A for different angles θ_{Bn}. For the limit of very high Mach numbers, this ratio approaches zero, which corresponds to zero deflection. For $\theta_{Bn} = 0$ and $\theta_{Bn} = \pi$, which corresponds to an upstream magnetic field parallel or perpendicular to the shock surface, the ratio is constant with the value zero.

Further, we can use equation (4.3.0.13) and find an expression for the downstream thermal velocity $\bar{v}$ in relation to the upstream bulk velocity V_u:

$$\frac{\bar{v}_d^2}{V_u^2} = \frac{1}{2r}\left[\frac{\beta_u}{M_A^2} + \frac{2(r-1)}{r} + \frac{\sin^2\theta_{Bn}}{M_A^2}\left(1 - \left(\frac{B_{dz}}{B_{uz}}\right)^2\right)\right]. \tag{4.3.0.23}$$

This ratio tells us about the rate, at which upstream bulk kinetic energy is converted into thermic energy at the shock front.
Next, we want to find the expression for the shock compression ratio r. The last two terms of equation (4.3.0.14) can be rewritten using equation (4.3.0.16), so they become

$$\frac{2V_{dx}B_{dz}^2}{\mu_0 m_i} - \frac{2V_{dz}B_x B_{dz}}{\mu_0 m_i} = \frac{2V_u B_{uz} B_{dz}}{\mu_0 m_i}. \tag{4.3.0.24}$$

Thus, we can combine equation (4.3.0.14) with the other equations above, which yields a quartic polynome in r. One solution is trivial for the case $r = 1$, which is not a shock-like solution, since there is no change of state. So, we end up with a cubic for the compression ratio r:

$$\begin{aligned} &\cos^2\theta_{Bn}(2M_A^2 + 5\beta_u\cos^2\theta_{Bn})r^3 \\ &\quad + M_A^2(M_A^2 - \cos^2\theta_{Bn}(5M_A^2 + 8 + 10\beta_u))r^2 \\ &\quad + M_A^4(11\cos^2\theta_{Bn} + 2M_A^2 + 5 + 5\beta_u)r - 8M_A^6 = 0 \end{aligned} \tag{4.3.0.25}$$

In the limit of high Mach numbers and upstream kinetic energies much larger than the magnetic or thermic energy, $M_A \longrightarrow \infty$ and $\beta_u \longrightarrow 0$, one can divide this polynome by M_A^6, which shows that the compression ratios maximal value is $r = 4$. Further, one sees that the ratio $\bar{v}_d/V_u$ from equation (4.3.0.23) is limited to the maximum value $\sqrt{3}/4$. The solutions for our shock conservation relations indicate that the high Mach number approximation is justified for $M_A = 5 - 10$.
These results have quite important physical interpretations: First, the limiting value for the compression ratio is identical to the limiting value for neutral fluids and completely independent of the electromagnetic properties of the system. Second, the limiting value for $\bar{v}_d/V_u$ tells us that bulk kinetic energy is converted to thermic energy very efficiently for high Mach numbers.

For solving the polynome (4.3.0.25) and thus deriving exact solutions for r, we distinguish between two different types of shocks:
Perpendicular shocks have $\theta_{Bn} = \pi/2$: The upstream magnetic field is parallel to the shock surface. The cubic polynome in r then reduces to a quadratic polynome that can easily be solved. The solution, that is physical and fulfills the condition $r > 0$, is

$$r = -\left(M_A^2 + \frac{5}{2}(\beta_u + 1)\right) + \left[\left(M_A^2 + \frac{5}{2}(\beta_u + 1)\right)^2 + 8M_A^2\right]^{\frac{1}{2}}. \tag{4.3.0.26}$$

As one can see, the compression ratio of the shock is influenced by the magnetic field as well as the thermal pressure, on which β_u depends.

On the other hand, *parallel shocks* have $\theta_{Bn} = 0$, thus the upstream magnetic field is directed perpendicular to the shock surface. Using this, we can factorize equation (4.3.0.25) and derive two different solutions for the value of r. One solution is $r = M_A^2$, where we have $B_{dz} \neq 0$ and $V_{dz} \neq 0$. The corresponding shock is called a switch-on shock, since the magnetic field and the bulk velocity acquire parallel components during their transition through the shock front.

The other type of shock has $B_{dz} = 0$ and a compression ratio of

$$r = \frac{4}{1 + 5\frac{\bar{v}_u^2}{V_u^2}}. \tag{4.3.0.27}$$

The higher the ratio $\bar{v}_u^2/V_u^2$, the smaller the compression ratio. This means that compression is more efficient, the more energy of the upstream fluid is bulk kinetic energy instead of thermal energy.

5 Conclusion and Outlook

Shock waves are an important feature of the interstellar medium, and supernova remnants are probably one of the most prominent examples for shocks in astrophysics. They are also of special importance for the study of cosmic rays, since they can accelerate electrons to relativistic energies.
The evolution of SNRs from a supernova explosion to its fading away into the ISM can be separated into three different phases: In the free expansion phase, the stellar ejecta of the SN propagate radially into the ISM with a constant velocity of $10^9\,\mathrm{cm\,s^{-1}}$ for a typical ejecta mass of $1\,\mathrm{M_\odot}$ and energy deposited in the ejecta of $10^{51}\,\mathrm{erg}$. These ejecta cause a shock wave in the ISM and thus heat it up to temperatures of about $10^6\,\mathrm{K}$. Once the remnant has swept up enough ambient mass, it slows down and enters the Sedov phase, where it expands adiabatically. In this phase, a reverse shock develops, which travels through the ejecta into the SNR, and the forward shock separates from the ejecta, since it propagates faster through the ISM than the ejected stellar material. Now the SNRs evolution only depends on its initial conditions and the properties of the ISM. For a typical density of interstellar gas of $1\,\mathrm{cm^{-3}}$, the Sedov phase begins after around 200 yr and at an SNR radius of 2.1 pc. Once the shock heated SNR gas slows down enough and cools down to app. $5 \times 10^5\,\mathrm{K}$, the remnant enters the radiative phase. The transitions happens after app. $3 \times 10^4\,\mathrm{yr}$ for the initial conditions mentioned above. In this phase, radiative cooling from metal lines dominates the further evolution of the remnant. It cools further during its $10^5\,\mathrm{yr}$ duration, until the SNRs fades away into the ambient gas.
At the forward shock front of an SNR, electrons are accelerated to relativistic energies and interact with the remnants magnetic field, thus emitting synchrotron radiation. The typical order of magnitude of an SNRs magnetic field is 100 mG. Synchrotron photons up to energies in the X-ray band correspond to electron energies of $10^{14}\,\mathrm{eV}$. Thus, SNRs could be an important source for cosmic rays. The mechanism of acceleration is probably diffusive shock acceleration, where charged particles are scattered from turbulences in the magnetic field and thus pass the forward shock front multiple times and acquiring kinetic energy each time. Due to lack of time, the physics of particle acceleration in the shock waves of SNRs could not be discussed in detail in this thesis. This would make a suitable topic for a further study, expanding on this one.

Based on the microscopic phase space distribution function $f(\boldsymbol{x}, \boldsymbol{p}, t)$ for the particles in a fluid, it was shown that macroscopic conservation laws can be derived for the mass (or particle number), the momentum and the energy of a fluid. This was done by taking the moments of the Boltzmann function, which describes the evolution of f. The method is equally feasible for neutral fluids and for collisionless plasmas. For neutral fluids it was

shown explicitly that a wave equation for sound waves can be derived. This wave equation can be solved via a linearization approach for small-scale perturbations, but for large-scale amplitudes non-linearities have to be considered. These non-linearities lead to the steepening of large-scale sound waves and thus the creation of shocks: Abrupt changes of state in the physical quantities of a fluid that are caused by a sudden transition from subsonic to supersonic flow. The jump conditions for these shocks show that the compression ratio, i.e. the change in density through the shock front, approaches a finite value for faster inflowing fluids, while the pressure and density ratio diverge.
For physical shocks, some sort of dissipative process is necessary to limit the steepening of a sound wave. In the case of collisional neutral fluids, this is provided by the viscosity resulting from the fluid particle's collisions. Without efficient particle collisions, which is usually the case in astrophysics, external force fields are necessary for allowing the creation of shocks. For the case of plasmas, these are the electromagnetic fields. Thus, plasmas are described by the Vlasov-Maxwell system of equations. As in the case of neutral fluids, macroscopic continuity equations and jump conditions for shock solutions can be derived. For the case of collisionless plasmas, these jump conditions are not uniquely defined and can only be solved if further assumptions about the considered plasma are made. Thus, there is a large amount of different shock solutions that can be found for actual astrophysical plasmas.
We considerer the special case of an electron-proton plasma with Maxwellian distribution and derived the jump conditions: The density compression ratio equals the one for neutral fluids in the limit of very fast shocks, as does the compression of the magnetic field tangential to the shock. We also derived that kinetic energy of the fluids bulk velocity is converted into thermal energy at the transition through the shock front.
Due to the complexity of the topic of shock waves in plasmas, a detailed study of different shock solutions was not possible within the scope of this thesis. Further analysis of this topic in a following study would be reasonable, especially due to the importance of the electromagnetic properties of the fluid for the mechanism of particle acceleration.

Besides the theoretical discussion of neutral fluids and collisionless plasmas and their shock solutions, another goal of this thesis was the adaption of S. Richter's and F. Spanier's *unicorn* code for SNRs. This code was programmed for numerical simulations of particle acceleration in the shock waves of the jets of active galactic nuclei. Due to the similarities between particle acceleration in AGNs and SNRs, it seems to be a reasonable goal to adapt the code's AGN parameters to the less extreme physical values of SNRs. So far, this approach did not yield useful results. More specifically, the calculated photon fluxes that would reach earth due to particle acceleration in an SNR were vanishingly small. For this reason, the results of the work with the unicorn code are not included in this thesis. Nevertheless, the goal of adopting the code for SNRs and performing numerical simulations of particle acceleration in SNRs stays desirable. It will be an element of further study.

Bibliography

Burgess, D. and Scholer, M. (2015). *Collisionless Shocks in Space Plasmas*. Cambridge University Press.

Dubner, G. and Giacani, E. (2015). Radio Emission from Supernova Remnants. *The Astronomy and Astrophysics Review*, 23(1).

Helder, E. A. et al. (2012). Observational Signatures of Particle Acceleration in Supernova Remnants. *Space Science Reviews*, 173(1-4):369–431.

Höfner, S. (2008). Lecture Notes: Astrofysikaliska dynamiska processer, The Equations of Fluid Dynamics and their Connection with the Boltzmann Equation. Department of Physics and Astronomy, Uppsala University.

Koyama, K. et al. (1995). Evidence for Shock Acceleration of High-energy Electrons in the Supernova Remnant SN1006. *Nature*, 378(6554):255–258.

Padmanabhan, T. (2000). *Theoretical Astrophysics: Volume 1, Astrophysical Processes*. Cambridge University Press.

Reynolds, S. P., Gaensler, B. M., and Bocchino, F. (2011). Magnetic Fields in Supernova Remnants and Pulsar-wind Nebulae. *Space Science Reviews*, 166(1-4):231–261.

Richter, S. and Spanier, F. (2016). A Numerical Model of Parsec-scale SSC Morphologies and their Radio Emission. *The Astrophysical Journal*, 829(1):56.

Sasaki, M. (2019). Lecture Notes: Interstellar Medium, Chapter 5: Hydrodynamics and Shock Waves. Dr. Karl Remeis Observatory, Erlangen Centre for Astroparticle Physics.

Seward, F. D. and Charles, P. A. (2012). *Exploring the X-ray Universe*. Cambridge University Press.

Soderberg, A. M. et al. (2008). An Extremely Luminous X-ray Outburst at the Birth of a Supernova. *Nature*, 453(7194):469–474.

Erklärung:

Hiermit bestätige ich, dass ich diese Arbeit selbstständig und nur unter Verwendung der angegebenen Hilfsmittel angefertigt habe.